Asynchronous Saturation of the Carbon Sink in African and Amazonian tropical forests

Wannes Hubau[1,2,3]*, Simon L. Lewis[1,4]*, Oliver L. Phillips[1], Kofi Affum-Baffoe[5], Hans Beeckman[2], Aida Cuni-Sanchez[4,6], Corneille E. N. Ewango[7,8,9], Sophie Fauset[1,10], Douglas Sheil[11,12,13], Bonaventure Sonké[14], Martin J. P. Sullivan[1], Terry Sunderland[15,16], Sean C. Thomas[17], Katharine A. Abernethy[18,19], Stephen Adu-Bredu[20], Christian A. Amani[21,22], Timothy R. Baker[1], Lindsay F. Banin[23], Fidèle Baya[24,25], Serge K. Begne[14,1], Amy C. Bennett[1], Fabrice Benedet[26], Robert Bitariho[12], Yannick E. Bocko[27], Pascal Boeckx[28], Patrick Boundja[29,13,30], Roel J.W. Brienen[1], Terry Brncic[29], Eric Chezeaux[31], George B. Chuyong[32], Connie J. Clark[33], Murray Collins[34], James A. Comiskey[35,36], David Coomes[37], Armandu K. Daniels[38], Greta C. Dargie[1], Thales de Haulleville[2,39], Marie Noel Djuikouo K.[14,40], Jean-Louis Doucet[41], Adriane Esquivel-Muelbert[1,42], Ted R. Feldpausch[43], Alusine Fofanah[44], Ernest G. Foli[20], Martin Gilpin[1], Emanuel Gloor[1], Christelle Gonmadje[45], Sylvie Gourlet-Fleury[26], Jefferson S. Hall [36], Alan Hamilton[46], David J. Harris[47], Terese B. Hart[48,49], Mireille B. N. Hockemba[29], Annette Hladik[50], Suspense A. Ifo[27], Kath Jeffery[51,52,53], Tommaso Jucker[54], Emmanuel Kasongo Yakusu[9,3,2], Elizabeth Kearsley[55,2], David Kenfack[36,56], Alexander Koch[4], Miguel E. Leal[57], Aurora Levesley[1], Jeremy A. Lindsell[58,59], Janvier Lisingo[60], Gabriela Lopez-Gonzalez[1], Jon C. Lovett[1,61], Jean-Remy Makana[60], Yadvinder Malhi[62], Andrew R. Marshall[63,64,65], Jim Martin[66], Emanuel Martin[56], Faustin M. Mbayu[9], Vincent P. Medjibe[67,53,33], Vianet Mihindou[53,68], Edward Mitchard[69], Sam Moore[62], Jacques M. Mukinzi [7,70,71], Pantaleo K.T. Munishi[72], Natacha Nssi Bengone[53], Lucas Ojo[73], Fidèle Evouna Ondo[53], Georgia C. Pickavance[1], Axel D. Poulsen[47], John R. Poulsen[33], Lan Qie[1], Jan Reitsma[74], Francesco Rovero[75,76], Michael D. Swaine[77], Hermann Taedoumg[14,78], Joey Talbot[1], James Taplin[79], David Taylor[80], Duncan W. Thomas[81], Benjamin Toirambe[82,2], John Tshibamba Mukendi[2,9,83], Darlington Tuagben[38], Peter M. Umunay[84,85], Hans Verbeeck[55], Jason Vleminckx[86,87], Lee J. T. White[53,19,88], Simon Willcock[89], Hannsjoerg Woell[90], John T. Woods[91], Lise Zemagho[14]

*Contributed equally

1. University of Leeds, School of Geography, Leeds, UK
2. Royal Museum for Central Africa, Service of Wood Biology, Tervuren, Belgium
3. Ghent University, Department of Environment, Laboratory of Wood Technology (Woodlab), Ghent, Belgium
4. University College London, Department of Geography, London, UK
5. Forestry Commission of Ghana, Mensuration Unit, Kumasi, Ghana
6. University of York, Department of Geography and Environment, York, UK
7. Wildlife Conservation Society, DR Congo Programme, Kinshasa, Democratic Republic of Congo
8. Centre de Formation et de Recherche en Conservation Forestiere (CEFRECOF), Epulu, Democratic Republic of Congo
9. Université de Kisangani, Faculté de Gestion de Ressources Naturelles Renouvelables, Kisangani, Democratic Republic of Congo
10. University of Plymouth, Plymouth, UK
11. Norwegian University of Life Sciences, Faculty of Environmental Sciences and Natural Resource Management, Ås, Norway
12. Mbarara University of Science and Technology (MUST), The Institute of Tropical Forest Conservation (ITFC) , Mbarara, Uganda
13. Center for International Forestry Research (CIFOR), Bogor, Indonesia
14. University of Yaounde I, Plant Systematic and Ecology Laboratory, Higher Teachers' Training College, Yaounde, Cameroon

15. Center for International Forestry Research (CIFOR), Sustainable Landscapes and Food Systems, Bogor, Indonesia
16. University of British Columbia, Faculty of Forestry, Vancouver, Canada
17. University of Toronto, Faculty of Forestry, Toronto, Canada
18. University of Stirling, Faculty of Natural Sciences, Stirling, UK
19. Institut de Recherche en Ecologie Tropicale, Libreville, Gabon
20. Forestry Research Institute of Ghana (FORIG), Kumasi, Ghana
21. Université Officielle de Bukavu, Bukavu, Democratic Republic of Congo
22. Center for International Forestry Research (CIFOR), Goma, Democratic Republic of Congo
23. Centre for Ecology and Hydrology, Penicuik, UK
24. Ministère des Eaux, Forêts, Chasse et Pêche (MEFCP), Bangui, Central African Republic
25. Institut Centrafricain de Recherche Agronomique (ICRA), Bangui, Central African Republic
26. Centre de coopération International en Recherche Agronomique pour le Développement (CIRAD), Forêts et Sociétés (F&S), Montpellier, France
27. Université Marien N'Gouabi, École Normale Supérieure (ENS), Département des Sciences et Vie de la Terre, Laboratoire de Géomatique et d'Ecologie Tropicale Appliquée, Brazzaville, Republic of Congo
28. Ghent University, Isotope Bioscience Laboratory-ISOFYS, Gent, Belgium
29. Wildlife Conservation Society, Congo Programme, Brazzaville, Republic of Congo
30. Resources and Synergies Development, Singapore, Singapore
31. Rougier-Gabon, Libreville, Gabon
32. University of Buea, Faculty of Science, Department of Plant and Animal Sciences, Buea, Cameroon
33. Duke University, Nicholas School of the Environment, Durham, NC, USA

34. Grantham Research Institute on Climate Change and the Environment, London, UK, London, UK
35. National Park Service, Inventory & Monitoring Program, Fredericksburg, VA, USA
36. Smithsonian Tropical Research Institute, Forest Global Earth Observatory (ForestGEO), Washington, DC, USA
37. University of Cambridge, Department of Plant Sciences, Cambridge, UK
38. Forestry Development Authority of the Government of Liberia (FDA), Monrovia, Liberia
39. University of Liège, Biodiversity and Landscape Unit, Liège, Belgium
40. University of Buea, Faculty of Science, Department of Botany and Plant Physiology, Buea, Cameroon
41. University of Liège, Forest Resources Management, Gembloux Agro-Bio Tech, Liège, Belgium
42. University of Birmingham, School of Geography, Earth and Environmental Sciences, Birmingham, UK
43. University of Exeter, Geography, College of Life and Environmental Sciences, Exeter, UK
44. The Gola Rainforest National Park, Kenema, Sierra Leone
45. National Herbarium, Yaounde, Cameroon
46. Kunming Institute of Botany, Kunming, China
47. Royal Botanic Garden Edinburgh, Edinburgh, UK
48. Lukuru Wildlife Research Foundation, Kinshasa, Democratic Republic of Congo
49. Yale Peabody Museum of Natural History, Division of Vertebrate Zoology, New Haven, CT, USA
50. Muséum National d'Histoire Naturel, Département Hommes, natures, sociétés, Paris, France
51. Institut de Recherche pour le Développement (IRD), Centre national de la recherche scientifique (CENAREST), Marseille, France

52. University of Stirling, Stirling, UK
53. Agence Nationale des Parcs Nationaux, Libreville, Gabon
54. CSIRO Land & Water, Floreat, Australia
55. Ghent University, Department of Environment, Computational & Applied Vegetation Ecology (Cavelab), Ghent, Belgium
56. Tropical Ecology, Assessment and Monitoring (TEAM) Network, Arlington, VA, USA
57. Wildlife Conservation Society, Uganda Programme, Kampala, Uganda
58. A Rocha International, Cambridge, UK
59. The Royal Society for the Protection of Birds, Centre of Conservation Science, Sandy, UK
60. Université de Kisangani, Faculté des Sciences, Laboratoire d'écologie et aménagement forestier, Kisangani, Democratic Republic of Congo
61. Royal Botanic Gardens, Kew, UK
62. University of Oxford, Environmental Change Institute, School of Geography and the Environment, Oxford, UK
63. University of York, Department of Environment and Geography, York, UK
64. University of the Sunshine Coast, Tropical Forests and People Research Centre, Sippy Downs, Australia
65. Flamingo Land Ltd, Kirby Misperton, UK
66. Fleming College, Peterborough, Canada
67. Central African Forests Commission (COMIFAC), Yaounde, Cameroon
68. Ministère de la Forêt, de l'environnement et de la Protection des Ressources Naturelles, Libreville, Gabon
69. University of Edinburgh, Edinburgh, UK
70. Salonga National Park, Kinshasa, Democratic Republic of Congo
71. World Wide Fund for Nature, Gland, Switzerland

72. Sokoine University of Agriculture, Morogoro, Tanzania
73. University of Abeokuta, Abeokuta, Nigeria
74. Bureau Waardenburg, Culemborg, The Netherlands
75. University of Florence, Department of Biology, Florence, Italy
76. MUSE - Museo delle Scienze, Tropical Biodiversity Section , Trento, Italy
77. University of Aberdeen, Department of Plant & Soil Science, School of Biological Sciences, Aberdeen, UK
78. Bioversity International, Yaounde, Cameroon
79. UK Research & Innovation, Innovate UK, London, UK
80. National University of Singapore, Department of Geography, Singapore, Singapore
81. Washington State University, Biology Department, Vancouver, WA, USA
82. Ministère de l'Environnement et Développement Durable, Kinshasa, Democratic Republic of Congo
83. Université de Mbujimayi, Faculté des Sciences Appliquées, Mbujimayi, Democratic Republic of Congo
84. Yale University, Yale School of Forestry & Environmental Studies, New Haven, CT, USA
85. Wildlife Conservation Society, New York, NY, USA
86. Université Libre de Bruxelles, Faculté des Sciences, Service d'Évolution Biologique et écologie, Brussels, Belgium
87. Florida International University, Department of Biological Sciences, Florida, FL, USA
88. University of Stirling, School of Natural Sciences, Stirling, UK
89. University of Bangor, School of Natural Sciences, Bangor, UK
90. Sommersbergseestrasse, Bad Aussee, Austria
91. University of Liberia, Monrovia, Liberia

Abstract

Structurally intact tropical forests sequestered ~50% of global terrestrial carbon uptake over the 1990s and early 2000s, offsetting ~15% of anthropogenic CO_2 emissions[1-3]. Climate-driven vegetation models typically predict that this tropical forest 'carbon sink' will continue for decades[4,5]. However, recent inventories of intact Amazonian forests show declining carbon sequestration[6]. Here, we assess the trends in African forests and compare with Amazonia. Records from 244 multi-census plots spanning 11 countries reveal that the carbon sink in aboveground live biomass in intact African tropical forests has been stable for the three decades to 2015, at 0.66 Mg C ha^{-1} yr^{-1} (95% CI: 0.53-0.79). Thus, the carbon sink responses of Earth's two largest expanses of tropical forest have diverged. As both continents show increasing tree growth (consistent with the expected net effect of rising atmospheric CO_2 and air temperature on photosynthesis and respiration[7]), the divergence arises from differences in carbon losses from tree mortality (no detectable multi-decadal trend in Africa; monotonic increase in Amazonia). Despite the past stability of the African carbon sink, our data suggest a very recent (*c.* 2010) increase in carbon losses, delayed compared to Amazonia, indicating asynchronous carbon sink saturation on the two continents. A statistical model including CO_2, temperature, drought, and forest dynamics can account for the observed trends. Extrapolating these predictor variables indicates a long-term decline in the African sink, being 18% smaller in 2030, while the Amazonian sink continues to rapidly weaken, reaching zero in the 2030s. Overall, the uptake of carbon into Earth's intact tropical forests peaked in the 1990s. Furthermore, this tropical sink is set to end decades sooner than even the most pessimistic vegetation models predict[4,5]. Observations indicating greater recent carbon uptake into the Northern hemisphere landmass[8] reinforce our conclusion that the intact tropical forest carbon sink has already saturated.

Main text

Tropical forests account for one-third of Earth's terrestrial Gross Primary Productivity and half of Earth's carbon stored in terrestrial vegetation[9]. Thus, small biome-wide changes in tree growth and mortality can have global impacts, either buffering or exacerbating the increase in atmospheric CO_2. Models[2,7,10], ground-based observations[11-13], airborne atmospheric CO_2 measurements[3,14], inferences from remotely sensed data[15], and synthetic approaches[3,16,17] each suggest that, after accounting for land-use change, remaining structurally intact tropical forests (i.e. not impacted by logging or fire) are increasing in carbon stocks. This structurally intact tropical forest 'carbon sink' is estimated at 1.2 Pg C yr^{-1} over 1990-2007 using inventory plot measurements[1]. Yet, despite its policy relevance, changes in this key carbon sink remain highly uncertain[18,19].

Rising CO_2 concentrations are thought to have boosted photosynthesis more than rising air temperatures have enhanced respiration, resulting in an increasing global terrestrial carbon sink[2,7,16,20]. Yet, for Amazonia, recent results from repeated censuses of intact forest inventory plots show a progressive two-decade decline in sink strength primarily due to an increase of carbon losses from tree mortality[6]. It is unclear if this simply reflects region-specific drought impacts[21,22], or potentially chronic pan-tropical impacts of either heat-related tree mortality[23] or internal forest dynamics resulting from past increases in carbon gains leaving the system[24]. A more recent deceleration of the rate of increase in carbon gains from tree growth is also contributing to the declining sink[6]. Again, it is not known if this is a result of either pan-tropical CO_2 fertilisation saturation or rising air temperatures, or is merely a regional drought impact. To address these uncertainties, we (i) analyze an unprecedented long-term inventory dataset from Africa, (ii) pool the new African and existing Amazonian records together to investigate the putative environmental drivers of changes in the tropical forest carbon sink, and (iii) project its likely future evolution.

We collected, compiled and analysed data from structurally intact old-growth forests from the African Tropical Rainforest Observation Network[25] (217 plots) and other sources (27 plots) spanning the period 1968 to 2015 (Extended Data Figure 1). In each plot (mean size, 1.1 ha), all trees ≥100 mm in stem diameter were identified, mapped and measured on at least two occasions using standardized methods (135,625 trees monitored) and live biomass carbon stocks were estimated for each census date, with carbon gains and losses calculated for each interval (Extended Data Figure 2).

We detect no long-term trend in the per unit area African tropical forest carbon sink over three decades to 2015 (Figure 1). The aboveground live biomass sink averaged 0.66 Mg C ha^{-1} yr^{-1} (95% CI: 0.53-0.79; n=244) and was significantly greater than zero for every year since 1990 (Figure 1). While very similar to past reports[11] (0.63 Mg C ha^{-1} yr^{-1}), this first estimate of the temporal trend in Africa contrasts with the Amazonian trend[6] (Figure 1). A linear mixed effect model shows a significant difference in the slopes of the sink trends for the two continents over the common time window (1983-2011.5; p=0.017). Thus, the per unit area sink strength of the two largest expanses of tropical forest on Earth have diverged.

The proximal cause of the divergent sink patterns is a significant increase in carbon losses (from tree mortality) in Amazonian forests, with no detectable trend over three decades in African forests (Figure 1). A linear mixed effects model shows a significant difference in slopes of carbon losses between the two continents over the common time window (p=0.027). Long-term trends in carbon gains (tree growth and newly recruited trees) are similar: we could detect no difference between the continents (Figure 1b; p=0.348). However, an assessment of how underlying environmental drivers affect carbon gains and losses is needed to understand the ultimate causes of the divergent sink patterns.

A linear mixed effects model of carbon gains, with censuses nested within plots, and pooling the new African and published Amazonian data, shows a significant positive relationship with CO_2, and significant negative relationships with mean annual temperature (MAT) and drought (measured as the Maximum Climatological Water Deficit, MCWD[12]; Figure 2; Extended Data Table 1). These results are consistent with a positive CO_2 fertilization effect, and negative effects of higher temperatures and drought on tree growth, consistent with temperature-dependent increases in autotrophic respiration, and temperature- and drought-dependent reductions in carbon assimilation. By contrast the equivalent model for carbon losses shows no significant relationships with CO_2, MAT or MCWD.

We further investigate the responses of carbon gains and losses (for which the above analysis has no explanatory power) by expanding our potential explanatory variables to include the environmental conditions during the census interval (CO_2, MAT and MCWD), the change in these conditions (CO_2-change, MAT-change, MCWD-change, see Extended Data Figure 3 for calculation details), and two forest attributes that may influence their response to the same environmental change: plot mean wood density (which in old-growth forests correlates with resource availability[26,27]), and the plot carbon residence time (which measures how long fixed carbon remains in the system, hence dictates when past increases in carbon gains leave the system as elevated carbon losses[28]).

The minimum adequate carbon gain model has a positive relationship with CO_2-change, and negative relationships with MAT, MAT-change, MCWD, and wood density (Table 2). The retention of both MAT and MAT-change suggests that higher temperatures correspond to lower tree growth, and that trees only partially acclimate to recently rising temperatures, which further reduces growth, consistent with warming experiments[29] and observations[30]. Given that lower carbon gains are related to higher wood density (Extended Data Figure 4) which shows no temporal trend (Extended Data Figure 5)

245 together suggests that old-growth forests with denser-wooded tree communities typically have fewer
246 available resources, consistent with expectations[24,26].
247
248 The minimum adequate carbon gain model using our expanded explanatory variables also highlights
249 continental differences. In Africa, from 2000 to 2015, carbon gains increased by 3.64% from CO_2-
250 change, but temperature rises led to a decline in gains of 0.24% (MAT and MAT-change together),
251 and increasing droughts further depleted gains by 0.51% (Table 2). For Amazonia, from 2000 to 2015,
252 gains increased by 3.68% due to CO_2-change (as in Africa), but temperature increases reduced gains
253 by 1.44% (six times the impact in Africa) while increasing droughts—and these forests' greater
254 sensitivity to drought—further reduced gains by 2.47% (five times the impact in Africa; Table 2).
255 Thus, the recent deceleration of carbon gains increase in Amazonia[6] is a response to drought and
256 temperature and not due to unexpected saturation of CO_2 fertilisation. Overall, the larger increase in
257 gains in Africa relative to Amazonia appear to be driven by slower warming, fewer droughts, lower
258 forest sensitivity to droughts, and overall lower temperatures (African forests are on average 1.1°C
259 cooler than Amazonian forests, as they typically grow at ~200 m higher elevation).
260
261 The minimum adequate carbon loss model using our expanded explanatory variables shows higher
262 losses with CO_2-change and MAT-change, and lower losses with MCWD and the carbon residence
263 time (CRT; Table 2). Changes in carbon losses appear to be largely a function of carbon gains. Firstly,
264 the greater losses in forests with shorter CRT conform to a 'high-gain high-loss' forest dynamics
265 pattern[24]. Secondly, wetter plots have a longer growing season and so have higher gains and
266 correspondingly higher losses, explaining the negative relationship with MCWD. Finally, as CO_2
267 results in additional carbon gains, after some time these additional past gains leave the system resulting
268 in greater carbon losses, explaining the positive relationship with CO_2-change. In addition to these
269 relationships with carbon gains, the inclusion of MAT-change ($p<0.001$) indicates heat- or Vapour

Pressure Deficit-induced tree mortality[23]. Overall, our results imply that chronic long-term environmental change factors, temperature and CO_2, rather than simply the direct effects of drought, underlie longer-term trends in tropical forest tree mortality.

The minimum adequate carbon loss model using our expanded explanatory variables replicates the divergent continental trends (Figure 3). The higher loss rates in Amazonia reflect the shorter CRT of Amazonian (56 yrs, 95% CI, 54-59) compared to African forests (69 yrs, 95% CI, 66-72), while the greater increase in loss rates in Amazonia results from faster warming and a shortening of CRT, which has been stable in African forests (Extended Data Figure 5). Furthermore, given that losses appear to lag behind gains they should relate to CRT. This is what we find: the longer the CRT the smaller the increase in carbon losses, with no increase in losses for plots with CRT ≥77 years (Extended Data Figure 6). Consequently, due to the typically longer residence times of African forests, increasing losses in Africa ought to appear 10-15 years after the increase in Amazon losses began (*c.*1995). Strikingly, in Africa the most recently monitored plots suggest that losses began increasing from *c.*2010 (Extended Data Figure 7), and plots with shorter CRT are driving the increase (Extended Data Figure 8).

Finally, our carbon gain and loss models can be used to estimate the future size of the per unit area intact forest carbon sink. Extrapolations of the changes in the predictor variables from 1983-2015 forward to 2040 (Extended Data Figure 5) show declines in the sink on both continents. By 2030 the carbon sink in aboveground live biomass in intact African tropical forest is predicted to decline from its 2010-15 mean by 18% (1σ range, 6-39%), to 0.54 Mg C ha^{-1} yr^{-1} (1σ range, 0.39-0.65). The Amazon sink is predicted to reach zero in 2034 (1σ range, 2023-2055; Figure 3). Thus, the carbon sink strength of the world's two most extensive tropical forests have now saturated, albeit asynchronously.

Together, our measurements and analyses signify that Earth recently passed the point of peak carbon sequestration into intact tropical forests (Table 1). The continental sink in Amazonia peaked in the 1990s and has declined since, driven by both reduced sink strength and forest area (Table 1; see Extended Data Table 2 for forest area). The African sink also peaked in the 1990s. In the 2000-10 decade the per ha sink peaked but was more than countered by continued forest area decline (Table 1). Including the modest uptake in the much smaller area of Asian tropical forest indicates that total pan-tropical carbon uptake peaked in the 1990s (Table 1). Given that the global terrestrial carbon sink has continued to increase, our results strongly imply that the extra-tropical terrestrial carbon sink has increased over the past two decades. Independent inter-hemispheric analyses of atmospheric CO_2 show Northern hemisphere forests have increased uptake over this time period[8].

In summary, while intact tropical forests remain key centres of biodiversity and major stores of carbon, our results show that their ability to sequester additional carbon is waning. Although tropical forests are more immediately threatened by deforestation and degradation, our analyses show that they are impacted by climate change. Given that no climate-driven vegetation model shows that peak net carbon uptake into intact tropical forests has already been passed[4,5], our analyses suggest that climate change impacts in the tropics may become more severe than predicted. Our findings also have political implications: as tropical forests are likely to sequester less carbon in the future than Earth System Models predict, an earlier date to reach net zero anthropogenic greenhouse gas emissions will be required to meet any given commitment to limit the global heating of Earth.

Acknowledgements

This paper is a product of the African Tropical Rainforest Observatory Network (AfriTRON), which only exists thanks to the kind support of governments, local administrations and villages across Africa who have given us permission for, and helped us complete, our fieldwork. We thank those in the places

we worked in Sierra Leone (Barrie, Gaura, Koya, Makpele, Malema, Nomo, Tunkia, Gola Rainforest National Park), Liberia (Garley town, River Gbeh, Glaro Freetown), Ghana (Asenanyo, Boekrom, Dadieso, Enchi, Dabiasem, Mangowase), Gabon (Ekobakoba, Mikongo, Babilone, Makokou, Leke/Moyabi Rougier Forestry Concession, Ivindo National Park, Lope National Park, Ipassa station, Kingele station, Tchimbele, Mondah, Ebe, Ekouk, Oveng, Sette Cama, Waka National Park), Cameroon (Nazareth, Lomié, Djomédjo, Alat-Makay, Somolomo, Deng Deng, Ejagham, Eyumojok, Mbakaou, Myere, Nguti, Bejange, Kekpane, Basho, Mendhi, Matene, Mboh, Takamanda, Obonyi, Ngoïla), Democratic Republic of Congo (Yoko, Yangambi, Monkoto) and Republic of Congo (Bomassa, Ekolongouma, Bolembe, Mbeli, Makao, Kabo, Niangui, Ngubu, Goualaki, Essimbi) for enabling the completion of censuses published for the first time here. For logistical and institutional support we thank the Forestry Department of the Government of Sierra Leone, the Conservation Society of Sierra Leone, the Royal Society for the Protection of Birds (RSPB), The Service de Coopération et d'Actions Culturelles (SCAC/MAE), Agence Française de Développement (AFD), University of Bangui, Société Centrafricaine de Déroulage (SCAD), Institut National pour l'Etude et la Recherche Agronomiques en R. D. Congo (INERA), Ecole Régionale Postuniversitaire d'Aménagement et de Gestion intégrés des Forêts et Territoires tropicaux (ERAIFT Kinshasa), the Ministère des Eaux et Forêts (République du Congo), the Ministère de la Rercherche Scientifique et de l'Innovation Technologique (République du Congo), the Nouabalé-Ndoki Foundation, WWF-D. R. Congo, Uganda Forest Department and the institutions of the co-authors. We thank the Centre de Coopération Internationale en Recherche Agronomique pour le Développement (CIRAD), the Tropical Ecology Assessment and Monitoring Network (TEAM), and the Forest Global Earth Observatory Network (ForestGEO) for access to data. Funding of AfriTRON data collection and this analysis: Natural Environment Research Council, the Royal Society, the Leverhulme Trust, the European Union FP7 GEOCARBON grant (to S.L.L), a Wolfson Merit Award (to O.P.P), and a European Research Council Advanced Grant to (O.L.P. and S.L.L. No. 291585; Tropical Forests in

the Changing Earth System, T-FORCES). W.H. was funded by T-FORCES and the Brain program of the Belgian Federal Government (BR/132/A1/AFRIFORD and BR/143/A3/HERBAXYLAREDD). A full list of acknowledgements is in Supplementary Notes.

Author Contributions

S.L.L. conceived the study and the AfriTRON forest plot re-census program. W.H., S.L.L., and O.L.P. developed the study. All authors, except M.S., R.B., E.G., A.L., G.L.-G., A.E.-M., A.K. and G.P., contributed data. W.H., M.S., S.L.L., O.L.P., R.B., A.L. G.L.-G., A.E.-M., A.K. and G.P. contributed analysis tools. W.H. and S.L.L. analysed the data. S.L.L. and W.H. wrote the paper, with all co-authors contributing to the manuscript.

Author Information (Materials & Correspondence)

Correspondence and requests for materials should be addressed to W.H. (w.hubau@gmail.com).

Competing interests

The authors declare no competing financial interests.

Data and code availability

Source data and R-code to generate figures and tables are available from: https://figshare.com/s/60f48673202283421f43.

Figures and Tables

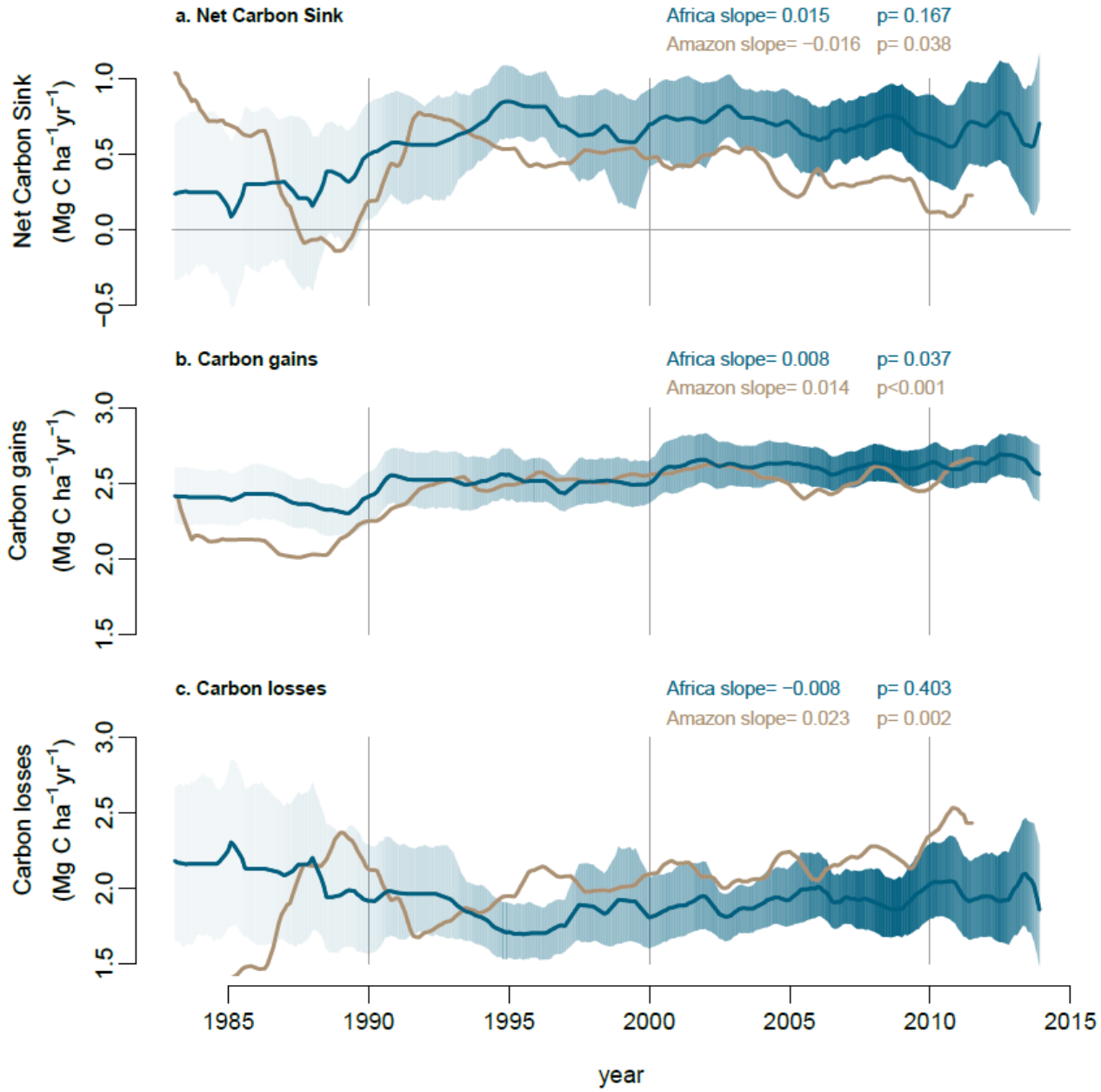

Figure 1. Long-term carbon dynamics of structurally intact tropical forests in Africa (blue) and Amazonia (brown). Trends in net aboveground live biomass carbon sink (**a**), carbon gains to the system from wood production (**b**), and carbon losses from the system from tree mortality (**c**), measured in 244 African inventory plots (blue lines) and contrasting published[6] Amazonian inventory data (brown lines; 321 plots). Shading corresponds to the 95% CI, with less transparent shading indicating a greater number of plots monitored in that year (most transparent: minimum 25 plots monitored). Printed slopes and p-values are from linear mixed effects models.

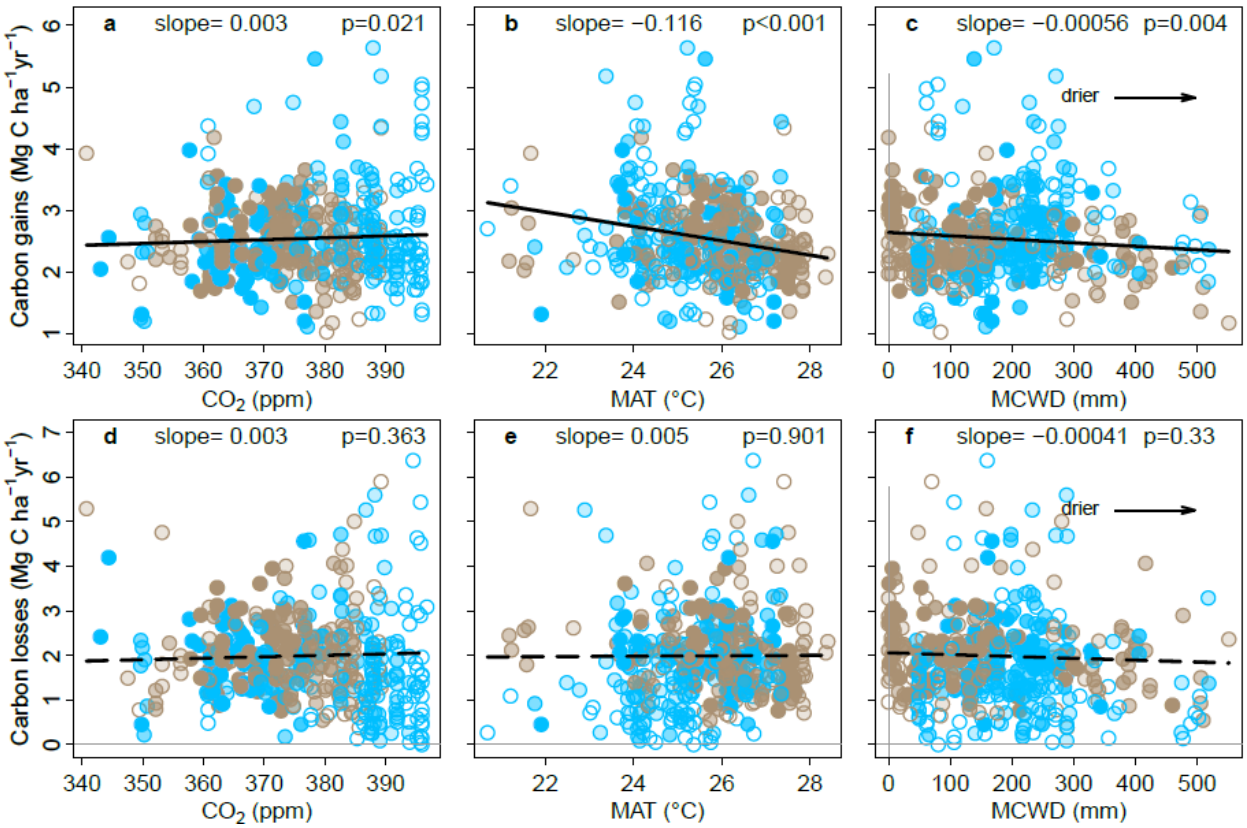

Figure 2. Potential environmental drivers of carbon gains and losses in structurally intact old-growth African and Amazonian tropical forests. The aboveground carbon gains, from woody productivity (**a-c**), and aboveground carbon losses, from mortality (**d-f**), are plotted as time-weighted plot-level mean values against the corresponding values of atmospheric carbon dioxide concentration (CO_2), mean annual air temperature (MAT) and drought (as Maximum Climatological Water Deficit, MCWD), for African (blue) and Amazonian (brown) inventory plots. Linear mixed effect models were performed with census intervals (n=1566) nested within plots (n=565), using an empirically derived weighting based on interval length and plot area (see methods); solid lines show significant regression lines for the complete dataset and non-significant regressions are shown as dashed lines. Transparency of the inner part of each data point represents total monitoring length, with empty circles corresponding to plots monitored for ≤ 5 years and solid dots for plots monitored for >20 years. Carbon loss data are presented untransformed for clarity; linear mixed effects models on data transformed to fit normality assumptions do not change the significance of the results (see Extended Data Table 1).

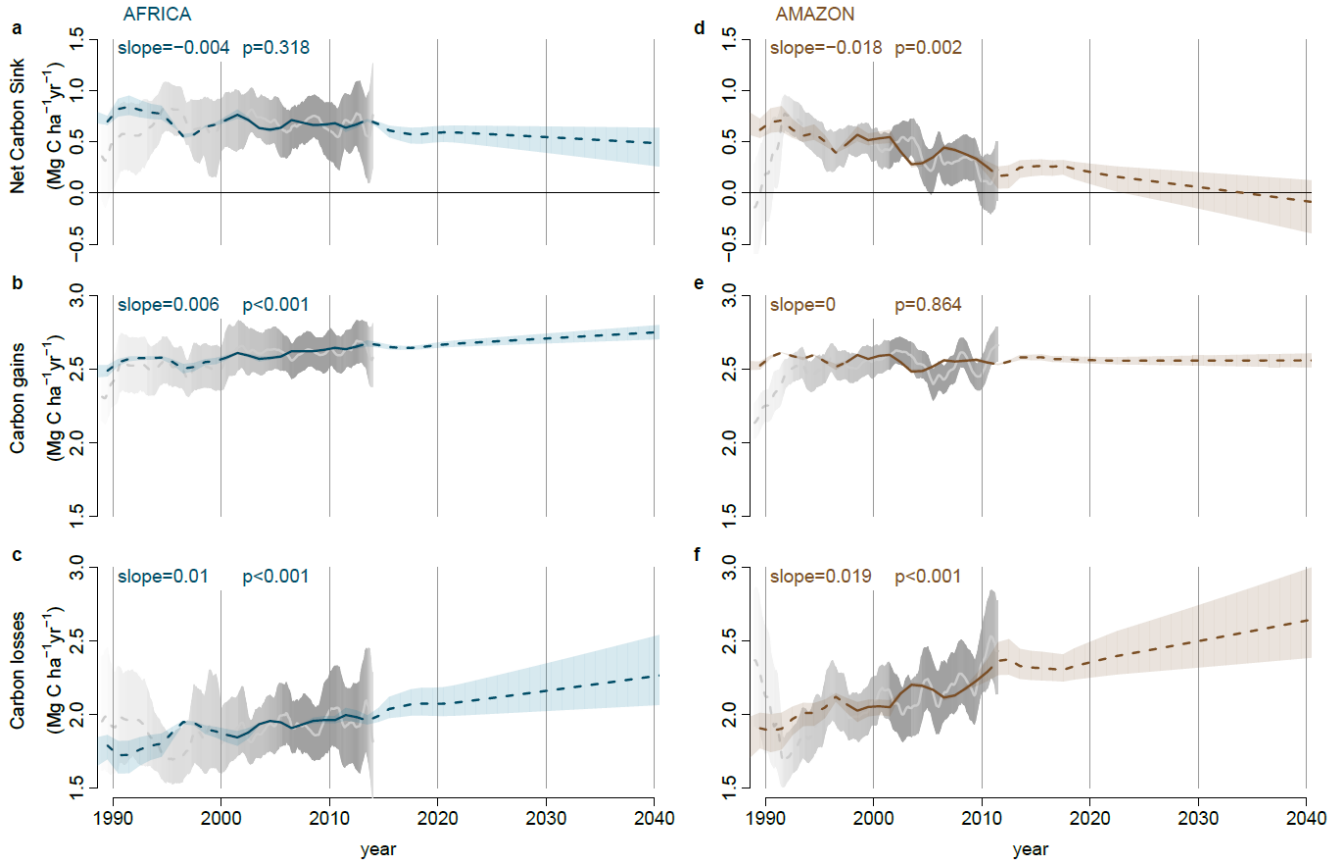

Figure 3. Modelled past and future carbon dynamics of structurally intact tropical forests in Africa and Amazonia. Predictions of net aboveground live biomass carbon sink (**a,d**), carbon gains (**b,e**), and carbon losses (**c,f**), for African (left panels) and Amazonian (right panels) plot inventory networks, based on CO_2-change, Mean Annual Temperature, Mean Annual Temperature-change, drought (as Maximum Climatological Water Deficit), plot wood density and plot carbon residence time. Model predictions are in blue (Africa) and brown (Amazon), with solid lines spanning the window when ≥75% of plots were monitored to show model consistency with the observed trends, and shading showing ±1σ uncertainty. Light grey lines and grey shading are from Fig.1, the mean observed and 95% CI of the observed trends.

Table 1. Carbon sink in intact forests in Africa, Amazonia and the pan-tropics: 1980-2015 and predictions to 2040 (in italics). Mean values in bold; in brackets 95% bootstrapped confidence intervals for the monitored period (1980-2015), and 2σ for the predictions (2010-2040).

Period	*n* (plots)		Per unit area aboveground C sink (Mg C ha^{-1} yr^{-1})		Total Continental C sink * (Pg C yr^{-1})		
	Af.	Am.	Africa	Amazon	Africa	Amazon	Pan-tropics †
1980-1990	45	73	**0.33** (0.06-0.63)	**0.35** (0.06-0.59)	**0.28** (0.05-0.53)	**0.49** (0.08-0.82)	**0.87** (0.17-1.53)
1990-2000	96	172	**0.67** (0.43-0.89)	**0.53** (0.42-0.65)	**0.50** (0.32-0.66)	**0.68** (0.54-0.83)	**1.26** (0.88-1.64)
2000-2010	194	291	**0.70** (0.55-0.84)	**0.38** (0.26-0.48)	**0.46** (0.37-0.56)	**0.45** (0.31-0.57)	**0.99** (0.70-1.25)
2010-2015	184	172	**0.66** (0.40-0.91)	**0.24** (0.00-0.47)	**0.40** (0.24-0.56)	**0.27** (0.00-0.52)	**0.73** (0.26-1.18)
2010-2020 ‡	-	-	***0.63*** *(0.49-0.69)*	***0.23*** *(0.13-0.30)*	***0.37*** *(0.29-0.41)*	***0.25*** *(0.14-0.33)*	***0.68*** *(0.45-0.83)*
2020-2030 ‡	-	-	***0.57*** *(0.28-0.70)*	***0.12*** *(-0.05-0.24)*	***0.30*** *(0.15-0.37)*	***0.12*** *(-0.05-0.24)*	***0.46*** *(0.11-0.68)*
2030-2040 ‡	-	-	***0.51*** *(0.06-0.72)*	***-0.02*** *(-0.28-0.16)*	***0.24*** *(0.03-0.34)*	***-0.02*** *(-0.26-0.15)*	***0.25*** *(-0.22-0.53)*

* Total Continental C sink is the per unit area aboveground C sink multiplied by intact forest area. Forest area is from ref.[1] for 1990, 2000 and 2010 (i.e. the total forest area minus forest regrowth); to estimate intact forest area for 1980, 2015, 2020, 2030 and 2040 we fitted exponential models for each continent using the 1990-2010 data. Total Continental C sink includes estimates of trees <100 mm DBH, lianas and roots, following ref.[11] for Africa and ref.[6] for Amazonia.

† Pan-tropical total carbon sink is the sum of African, Amazonian and Southeast Asian total continental carbon sink values. Southeast Asian values were estimated from forest area from ref.[1] and published per unit area carbon sink data[13] (n=49 plots) for 1990-2015, with 1980-1990 assumed to be the same as 1990-2000 due very low sample sizes. The sink in Southeast Asia has been a modest and declining contribution to the pan-tropical sink, at 0.12, 0.09 and 0.08 Pg C yr^{-1} in the 1980s, 1990s, and 2000s.

‡ Per unit area total C sink for 2010-2020, 2020-2030 and 2030-2040 was predicted using parameters from Table 2, except for the sink in Asia we assumed the parameters as for Africa, as Asian forest median CRT is 61 years, close to African median, 63 years.

458 **Table 2. Minimum adequate models to predict carbon gains and losses in African and**
459 **Amazonian tropical forests.** Where continental values differ, those for Africa are reported first,
460 followed by Amazonian values.

Carbon gains, Mg C ha^{-1} yr^{-1}					
Predictor variable	**Parameter value**	**Standard Error**	**t-value**	**p-value**	**2000-2015 change in gains (%) ***
(Intercept)	5.400 | 5.530	0.592 | 0.599	9.121 | 9.236	<0.001 | <0.001	-
CO_2-change (ppm yr^{-1})	0.234	0.096	2.429	0.015	3.64% | 3.68%
MAT (°C)	-0.087	0.025	-3.463	0.001	-0.76% | -1.14%
MAT-change (°C yr^{-1})	-0.766	0.189	-4.051	<0.001	0.52% | -0.3%
MCWD (mm x1000)	-0.411 | -1.381	0.376 | 0.239	-1.091 | -5.787	0.275 | <0.001	-0.51% | -2.47%
Wood Density (g cm^{-3})	-1.350	0.527	-2.561	0.011	0.05% | 0.00%
Carbon losses, Mg C ha^{-1} yr^{-1} †					
Predictor variable	**Parameter value**	**Standard Error**	**t-value**	**p-value**	**2000-2015 change in losses (%) ***
(Intercept)	1.213	0.087	13.931	<0.001	-
CO_2-change (ppm yr^{-1})	0.125	0.059	2.135	0.033	13.29% | 11.95%
MAT-change (°C yr^{-1})	0.478	0.130	3.673	<0.001	-1.73% | 0.89%
MCWD (mm x1000)	-0.218	0.107	-2.042	0.041	-1.33% | -1.74%
CRT (yr)	-0.003	0.001	-5.913	<0.001	-0.68% | 1.14%

461 * The 2000-2015 change in gains/losses for each predictor variable was estimated allowing only the focal
462 predictor to vary; this change was then expressed as a percentage of the annual gains/losses in the year 2000
463 allowing all predictors to vary.

464 † carbon loss values were normalized via power-law transformation, $\lambda = 0.361$.

References

1 Pan, Y. *et al.* A Large and Persistent Carbon Sink in the World's Forests. *Science* **333**, 988-993, doi:10.1126/science.1201609 (2011).

2 Sitch, S. *et al.* Recent trends and drivers of regional sources and sinks of carbon dioxide. *Biogeosciences* **12**, 653-679, doi:10.5194/bg-12-653-2015 (2015).

3 Gaubert, B. *et al.* Global atmospheric CO_2 inverse models converging on neutral tropical land exchange, but disagreeing on fossil fuel and atmospheric growth rate. *Biogeosciences* **16**, 117-134, doi:10.5194/bg-16-117-2019 (2019).

4 Huntingford, C. *et al.* Simulated resilience of tropical rainforests to CO_2-induced climate change. *Nature Geoscience* **6**, 268-273, doi:10.1038/ngeo1741 (2013).

5 Mercado, L. M. *et al.* Large sensitivity in land carbon storage due to geographical and temporal variation in the thermal response of photosynthetic capacity. *New Phytologist* **218**, 1462-1477, doi:doi:10.1111/nph.15100 (2018).

6 Brienen, R. J. W. *et al.* Long-term decline of the Amazon carbon sink. *Nature* **519**, 344-348, doi:10.1038/nature14283 (2015).

7 Piao, S. *et al.* Evaluation of terrestrial carbon cycle models for their response to climate variability and to CO2 trends. *Global Change Biology* **19**, 2117-2132, doi:10.1111/gcb.12187 (2013).

8 Ciais, P. *et al.* Five decades of northern land carbon uptake revealed by the interhemispheric CO_2 gradient. *Nature*, doi:10.1038/s41586-019-1078-6 (2019).

9 Lewis, S. L., Edwards, D. P. & Galbraith, D. Increasing human dominance of tropical forests. *Science* **349**, 827-832, doi:10.1126/science.aaa9932 (2015).

10 Pugh, T. A. M. *et al.* Role of forest regrowth in global carbon sink dynamics. *Proceedings of the National Academy of Sciences* **116**, 4382-4387, doi:10.1073/pnas.1810512116 (2019).

11 Lewis, S. L. *et al.* Increasing carbon storage in intact African tropical forests. *Nature* **457**, 1003-1006, doi:10.1038/nature07771 (2009).

12 Phillips, O. L. *et al.* Drought sensitivity of the Amazon rainforest. *Science* **323**, 1344-1347, doi:10.1126/science.1164033 (2009).

13 Qie, L. *et al.* Long-term carbon sink in Borneo's forests halted by drought and vulnerable to edge effects. *Nature Communications* **8**, 1966, doi:10.1038/s41467-017-01997-0 (2017).

14 Gatti, L. V. *et al.* Drought sensitivity of Amazonian carbon balance revealed by atmospheric measurements. *Nature* **506**, 76-80, doi:10.1038/nature12957 (2014).

15 Baccini, A. *et al.* Tropical forests are a net carbon source based on aboveground measurements of gain and loss. *Science* **358**, 230-234, doi:10.1126/science.aam5962 (2017).

16 Schimel, D., Stephens, B. B. & Fisher, J. B. Effect of increasing CO_2 on the terrestrial carbon cycle. *Proceedings of the National Academy of Sciences* **112**, 436-441, doi:10.1073/pnas.1407302112 (2015).

17 Keenan, T. F. *et al.* Recent pause in the growth rate of atmospheric CO_2 due to enhanced terrestrial carbon uptake. *Nature Communications* **7**, 13428, doi:10.1038/ncomms13428 (2016).

18 Booth, B. B. B. *et al.* High sensitivity of future global warming to land carbon cycle processes. *Environmental Research Letters* **7**, 024002 (2012).

19 Lombardozzi, D. L., Bonan, G. B., Smith, N. G., Dukes, J. S. & Fisher, R. A. Temperature acclimation of photosynthesis and respiration: A key uncertainty in the carbon cycle-climate feedback. *Geophysical Research Letters* **42**, 8624-8631, doi:doi:10.1002/2015GL065934 (2015).

20 Le Quéré, C. *et al.* Global Carbon Budget 2018. *Earth Syst. Sci. Data* **10**, 2141-2194, doi:10.5194/essd-10-2141-2018 (2018).

513 21 Lewis, S. L., Brando, P. M., Phillips, O. L., van der Heijden, G. M. F. & Nepstad, D. The 2010
514 Amazon drought. *Science* **331**, 554 (2011).
515 22 Feldpausch, T. R. *et al.* Amazon forest response to repeated droughts. *Global Biogeochemical*
516 *Cycles* **30**, 964-982, doi:doi:10.1002/2015GB005133 (2016).
517 23 Lewis, S. L. *et al.* Concerted changes in tropical forest structure and dynamics: evidence from
518 50 South American long-term plots. *Philosophical Transactions of the Royal Society of London*
519 *Series B-Biological Sciences* **359**, 421-436 (2004).
520 24 McDowell, N. *et al.* Drivers and mechanisms of tree mortality in moist tropical forests. *New*
521 *Phytologist* **219**, 851-869, doi:doi:10.1111/nph.15027 (2018).
522 25 Lewis, S. L. *et al.* Above-ground biomass and structure of 260 African tropical forests.
523 *Philosophical Transactions of the Royal Society B: Biological Sciences* **368**, 20120295-
524 20120295, doi:10.1098/rstb.2012.0295 (2013).
525 26 Quesada, C. A. *et al.* Basin-wide variations in Amazon forest structure and function are
526 mediated by both soils and climate. *Biogeosciences* **9**, 2203-2246, doi:10.5194/bg-9-2203-
527 2012 (2012).
528 27 Malhi, Y. *et al.* The above-ground coarse wood productivity of 104 Neotropical forest plots.
529 *Global Change Biology* **10**, 563-591 (2004).
530 28 Galbraith, D. *et al.* Residence times of woody biomass in tropical forests. *Plant Ecology &*
531 *Diversity* **6**, 139-157, doi:10.1080/17550874.2013.770578 (2013).
532 29 Reich, P. B. *et al.* Boreal and temperate trees show strong acclimation of respiration to
533 warming. *Nature* **531**, 633-636, doi:10.1038/nature17142 (2016).
534 30 Anderegg, W. R. L. *et al.* Tropical nighttime warming as a dominant driver of variability in the
535 terrestrial carbon sink. *Proceedings of the National Academy of Sciences* **112**, 15591-15596,
536 doi:10.1073/pnas.1521479112 (2015).
537

Methods

Plot selection

Closed canopy (i.e. not woody savanna) old-growth mixed-age forest inventory plots were selected using commonly used criteria[6,11,25]: free of fire and industrial logging; all trees with diameter at reference height ≥100 mm measured at least twice; ≥0.2 ha area; <1500 m.a.s.l. altitude; MAT ≥20.0°C[31]; annual precipitation ≥1000 mm[31] ; located ≥50 m from anthropogenic forest edges. Of the 244 plots included in the study, 217 contribute to the African Tropical Rainforest Observatory Network (AfriTRON; www.afritron.org), with data curated at www.ForestPlots.net. These include plots from Sierra Leone, Liberia, Ghana, Nigeria, Cameroon, Gabon, Republic of Congo, Democratic Republic of Congo (DRC), Uganda and Tanzania[32] (Extended Data Figure 1). Fifteen plots are part of the TEAM network, from Cameroon, Republic of Congo, Tanzania, and Uganda[33-36]. Nine plots contribute to the ForestGEO network, from Cameroon and DRC[37] (9 plots from DRC, codes SNG, contribute to both AfriTRON and ForestGEO networks, included above in the AfriTRON total). Finally, three plots from Central African Republic are part of the CIRAD network[38]. The large majority of plots are sited in terra firme forests and have mixed species composition, although four are in seasonally flooded forest and 14 plots are in *Gilbertiodendron dewevrei* monodominant forest, a locally common forest type in Africa (Supplementary Table 1). The 244 plots have a mean size of 1.1 ha (median, 1 ha), with a total plot area of 277.9 ha. The dataset comprises 391,968 diameter measurements on 135,625 stems, of which 89.9% were identified to species, 97.5% to genus and 97.8% to family. Mean total monitoring period is 11.8 years, mean census length 5.7 years, with a total of 3,214 ha years of monitoring. The 321 Amazon plots are published and were selected using the same criteria[6], except in the African selection criteria we specified a minimum anthropogenic edge distance and added a minimum temperature threshold.

563 **Plot inventory and Tree Biomass Carbon Estimation**

564 Tree-level aboveground biomass carbon is estimated using an allometric equation with parameters for
565 tree diameter, tree height and wood mass density. The estimated aboveground biomass of a plot is the
566 sum of the estimated biomass of all live trees at that census date.

567

568 *Tree Diameter:* In all plots, all woody stems with ≥100 mm diameter at 1.3 m from the base of the
569 stem ('diameter at breast height', DBH), or 0.5 m above deformities or buttresses, were measured,
570 mapped and identified using standard forest inventory methods[39]. The height of the point of
571 measurement (POM) was marked on the trees and recorded, so that the same POM is used at the
572 subsequent forest census. For stems developing deformities or buttresses over time that could
573 potentially disturb the initial POM, the POM was raised approximately 500 mm above the deformity.
574 Estimates of the diameter growth of trees with changed POM used the ratio of new and old POMs, to
575 create a single trajectory of growth from the series of diameters at two POM heights[6,11,40]. We used
576 standardized protocols to assess typographical errors and potentially erroneous diameter values (e.g.
577 trees shrinking by >5 mm), missing values, failures to find the original POM, and other issues. Where
578 necessary we estimated the likely value via interpolation or extrapolation from other measurements of
579 that tree, or when this was not possible we used the median growth rate of trees in the same plot, census
580 and size-class, defined as DBH = 100-199 mm, or 200-399 mm, or >400 mm[32,41]. We interpolate
581 measurements for 1.3% of diameters, extrapolate 0.9%, and use median growth rates for 1.5%.

582

583 *Tree height*: Height of individuals from ground to the top leaf, hereafter H_t, was measured in 204 plots,
584 using a laser hypsometer (Nikon forestry Pro) from directly below the crown (most plots), a laser or
585 ultrasonic distance device with an electronic tilt sensor, a manual clinometer, or by direct
586 measurement, i.e. tree climbing. Only trees where the top was visible were selected[42]. In most plots,
587 tree selection was similar: the 10 largest trees were measured, together with 10 randomly selected trees

per diameter from five classes: 100-199 mm, 200-299 mm, 300-399 mm, 400-499 mm, and 500+ mm trees, following standard protocols[42]. We use these data and the local.heights function in R package BiomasaFP[43] to fit 3-parameter Weibull relationships:

$H_t = a \times (1 - e^{\left(-b \times \left(\frac{DBH}{10}\right)^c\right)})$ (equation 1).

We chose the Weibull model as it is known to be robust when a large number of measurements are available[42,44]. We parameterize this H_t-DBH relationship for terra firme forest in three biogeographical regions, parameters in parentheses: (i) West Africa (a=56.0; b=0.0401; c=0.744); (ii) Lower Guinea and Western Congo Basin (a=47.6; b=0.0536; c=0.755); (iii) Eastern Congo Basin and East Africa (a=50.8; b=0.0499; c=0.706); and finally (iv) for seasonally flooded forest from Lower Guinea and Western Congo Basin (a=38.2; b=0.0605; c=0.760; there were no seasonally flooded forest plots in the other regions). The parameters were used to estimate H_t from DBH for all tree DBH measurements for input into the allometric equation.

Wood Density: Dry wood density (ρ) measurements were compiled for 730 African species from published sources and stored in www.ForestPlots.net; most were sourced from the Global Wood Density Database on the Dryad digital repository (www.datadryad.org)[45,46]. Each individual in the tree inventory database was matched to a species-specific mean wood density value. Species in both the tree inventory and wood density databases were standardized for orthography and synonymy using the African Flowering Plants Database (www.ville-ge.ch/cjb/bd/africa/) to maximize matches[11]. For incompletely identified individuals or for individuals belonging to species not in the ρ database, we used the mean ρ value for the next higher known taxonomic category (genus or family, as appropriate). For unidentified individuals, we used the mean wood density value of all individual trees in the plot[11,32].

612 *Allometric equation:* For each tree we use a published allometric equation[47] to estimate aboveground
613 biomass. We then convert this to carbon, assuming that aboveground carbon (AGC) is 45.6% of
614 aboveground biomass[48]. Thus: $AGC = 0.456 \times ((0.0673 \times (\rho \times \left(\frac{DBH}{10}\right)^2 \times H_t)^{0.976})/1000)$
615 (equation 2), with DBH in mm, dry wood density, ρ, in g cm^{-3}, and total tree height, H_t, in m (ref.[47]).
616
617 **Aboveground biomass carbon, carbon gains and carbon losses**
618 *Aboveground Carbon* (AGC, in Mg C ha^{-1}) in living biomass for each plot at each census date was
619 estimated as the sum of the AGC of each living stem, then divided by plot area (in hectares).
620
621 *Carbon Gain* is the sum of the aboveground live biomass carbon additions from the growth of
622 surviving stems and the addition of newly recruited stems, using standard methods[6]. For each stem
623 that survived a census interval, carbon additions from its growth (Mg C ha^{-1} yr^{-1}) were calculated as
624 the difference between its AGC at the end census of the interval and its AGC at the beginning census
625 of the interval. For each stem that recruited during the census interval (i.e. reaching DBH≥100 mm),
626 carbon additions were calculated in the same way, assuming DBH=0 mm at the start of the interval[40].
627 The carbon additions in an interval, from surviving and newly recruited stems, were summed, then
628 divided by the census interval length (in years), and scaled by plot area (in hectares)[40]. As carbon gains
629 are affected by a census interval bias, with the underestimate increasing with census length, we
630 corrected this bias by accounting for (i) the carbon additions from trees that recruited and then died
631 within the same interval (unobserved recruitment), and (ii) the carbon additions from trees that grew
632 before they died within an interval (unobserved growth)[40]. These typically add <3% to plot-level
633 carbon gains.
634
635 *Carbon Loss* (in Mg C ha^{-1} yr^{-1}) is estimated, using standard methods[6], as the sum of aboveground
636 biomass carbon from all stems that died during a census interval, divided by the census length (in

637 years) and scaled by plot area (in hectares). Carbon loss is also affected by the same census interval
638 bias, hence we corrected this bias by accounting for (i) the additional carbon losses from the trees that
639 were recruited and then died within the same interval, and (ii) the additional carbon losses resulting
640 from the growth of the trees that died in the interval[6,13,43].
641
642 *Net Carbon Sink* (in Mg C ha^{-1} yr^{-1}) is estimated as carbon gains minus carbon losses. All calculations
643 were performed using the R statistical platform, version 3.2.1[49] using the BiomasaFP R package
644 v0.2.1[43].
645
646 **Long-term gain, loss and net carbon sink trends estimation**
647 The estimated mean carbon gains, carbon losses and the net carbon sink of the African plots from
648 1983-2014, the solid lines in Figure 1, were calculated following ref.[6] to allow direct comparison with
649 published Amazonian results. First, each census interval value was interpolated for each 0.1-yr period
650 within the census interval. Then, for each 0.1-yr period between 1983 and 2014, we calculate a
651 weighted mean of all plots monitored at that time, using the square root of plot area as a weighting
652 factor[6]. Finally, confidence intervals for each 0.1-yr period are bootstrapped. The means and
653 confidence intervals shown in Extended Data Figure 7 and Extended Data Figure 8 were also
654 calculated using this method.
655
656 Trends in carbon gains, losses and the net carbon sink over time were assessed using linear mixed
657 effects models (lmer function in R, lme4 package[50]), providing the linear slopes reported in Figure 1.
658 These models regress the mid-point of each census interval against the value of the response variable
659 for that census interval. Plot identity was included as a random effect, i.e. assuming that the intercept
660 can vary randomly among plots. Observations were weighted by plot size and census interval length.
661 Weightings were derived empirically, by assuming *a priori* that there is no significant relation between

662 the net carbon sink and census interval length or plot size[11]. The following weighting removes all
663 pattern in the residuals:

664 $Weight = \sqrt[3]{length_{int}} + \sqrt[4]{plotsize} - 1$ (equation 3),

665 where $length_{int}$ is the length of the census interval, in years. Significance was assessed by regressing
666 the residuals of the net carbon sink model against the weights (p=0.702).

667

668 Differences in long-term slopes between the two continents for carbon gains, carbon losses and net
669 carbon sink were assessed using linear mixed effects models, as described above, but performed on
670 the combined African and Amazonian datasets and limited to their common time window, 1983 to
671 2011.5. These models had an interaction term between census interval date and continent, where a
672 significant interaction would indicate that the slopes differ between continents. The statistical
673 significance of continental differences in slope were assessed using the F-statistic (Anova function in
674 R, car package[51]).

675

676 **Continental and pan-tropical carbon sink estimates**

677 For Africa, Amazonia and Southeast Asia, we calculate the continental-scale total carbon sink (Pg C
678 yr^{-1}) for each decade between 1980 and 2010 and for 2010-2015 (Table 1). We do this by multiplying
679 the per unit area total net carbon sink (in Mg C ha^{-1} yr^{-1}; using all plots monitored in each of the time
680 intervals), by the area of intact forest on each continent at that time interval (in ha).

681

682 For each time period we calculate the per unit area *aboveground* net carbon sink in living trees with
683 DBH≥100 mm (expressed in Mg C ha^{-1} yr^{-1}) as the mean of all plot-level values, using plots for which
684 census dates overlap the time window, with plots weighted by the square root of plot area (as for the
685 solid lines in Figure 1). For plots with more than one census interval within the target time window,
686 the time-weighted average of the intervals was used. For Africa we use the per unit area net carbon

687 sink values presented in this paper. For Amazonia, we use data presented in this paper and previously
688 published in ref.[6]. For Southeast Asia, we use inventory data collected using similar standardized
689 methods, for 49 plots in ref.[13]. However there is a lack of Asian data covering 1980-1990, so we assume
690 that the per unit area net carbon sink for this decade is the same as for 1990-2000. We then calculate
691 the per unit area *total* carbon sink (in Mg C ha^{-1} yr^{-1}) for each period, as the sum of (i) the per unit area
692 *aboveground* carbon sink from large living trees and lianas with DBH≥100 mm; (ii) the per unit area
693 *aboveground* carbon sink from living trees and lianas with DBH<100 mm (5.19%, 9.40% and 5.46%
694 of carbon of large living trees in Africa, Amazonia and Southeast Asia respectively[52]); and (iii) the per
695 unit area *belowground* carbon sink in live biomass, i.e. roots (assuming belowground carbon is 25%,
696 37% and 17% of aboveground carbon of large living trees in Africa[11], Amazonia[6] and Southeast Asia[53]
697 respectively).
698
699 For comparability with previous continental-sink results, we used continental values of intact forest
700 area for 1990, 2000 and 2010 as published in ref.[1], *i.e.* total forest area minus forest regrowth. We used
701 the 1990-2010 data to fit an exponential model for each continent and used this model to estimate
702 intact forest area for 1980 and 2015 (Extended Data Table 2). The continent-level total carbon sink
703 (Pg C ha^{-1} yr^{-1}) for each period is the total per unit area total carbon sink (in Mg C ha^{-1} yr^{-1}) scaled by
704 the area of remaining intact tropical forest (in ha).
705
706 **Predictor variables**
707 We examined potential predictor variables for each census interval of each plot that may explain the
708 long-term trends in carbon gains and carbon losses. First, the environmental conditions during the
709 census interval; second the rate of change of these parameters; and third forest attributes that may
710 affect how different forests respond to the same environmental change. The predictor variable
711 estimates for each census need to avoid bias due to seasonal variation, for example the intra-annual

712 variability in atmospheric CO_2 concentration. We therefore applied the following procedure to avoid
713 seasonal variability impacts on long-term trends: (i) the length of each focal census interval was
714 rounded to the nearest complete year (e.g. a 1.1 year interval became a 1 year interval); (ii) we
715 computed dates that minimised the difference between actual fieldwork dates and complete-year
716 census dates, while ensuring that subsequent census intervals of a plot do not overlap. The resulting
717 sequence of non-overlapping census intervals was used to calculate interval-specific means for each
718 environmental predictor variable to remove seasonal effects. The average difference between the actual
719 fieldwork dates and the complete-year census dates is 0.01 decimal years (i.e. less than one week).
720
721 The first group of potential predictor variables, estimated for each census interval of each plot, are
722 theory-driven choices: atmospheric CO_2 concentration (CO_2), mean annual temperature (MAT), and
723 drought intensity, which we quantified as maximum climatological water deficit (MCWD)[54].
724 *Atmospheric CO_2 concentration* (CO_2, in ppm) is estimated as the mean of the monthly mean values
725 from the Mauna Loa record[55] over the census interval (corrected to avoid seasonality effects). While
726 atmospheric CO_2 concentration is highly correlated with time (R^2=0.98), carbon gains are slightly
727 better correlated with CO_2, as expected.
728
729 *Mean Annual Temperature* (MAT, in °C) was derived from a combination of the fine-scale (~1 km²
730 resolution) static WorldClim dataset[31] and the coarser scale (~3025 km² resolution) temporally
731 resolved Climatic Research Unit dataset (CRU TS 3.23)[56]. For each plot, we first extracted the monthly
732 mean temperature record covering 1901-2015 from the CRU dataset and calculated mean annual
733 temperature (MAT) over that period. Then we multiplied each value in the monthly CRU record by
734 the ratio of the WorldClim-MAT and the CRU-MAT. We then calculated MAT for each census
735 interval of each plot using the adjusted monthly CRU record.
736

737 *Maximum Climatological Water Deficit* (MCWD, in mm) was derived from a combination of the fine-
738 scale (~1 km^2 resolution) static WorldClim precipitation dataset[31] and the coarser scale (~3025 km^2
739 resolution) temporally resolved Global Precipitation Climatology Centre dataset (GPCC) that includes
740 many more gauges than CRU in tropical Africa[57,58] following a similar approach as to MAT. However,
741 as GPCC ends in 2013 we combined it with satellite-based Tropical Rainfall Measurement Mission
742 data (TRMM 3B43 V7 product, 0.25^o resolution)[59]. The fit for the overlapping time period (1998-
743 2013) was used to correct the systematic difference between GPCC and TRMM: GPCC' = a+b*GPCC,
744 with GPCC' the adjusted GPCC record and a and b different parameters for each month of the year
745 and for each continent. For each plot, we first extracted the monthly precipitation record covering
746 1901-2015 from the adjusted GPCC dataset and calculated mean monthly precipitation over that
747 period. Then we multiplied each value in the monthly GPCC record by the ratio of the WorldClim
748 mean monthly precipitation to the GPCC mean monthly precipitation. Then for each census interval
749 we extract monthly precipitation values and calculate monthly Climatological Water Deficit (CWD),
750 which is a commonly used metric of dry season intensity for tropical moist forests[12,20,54]. To avoid
751 intra-annual variability, monthly CWD values are calculated for each subsequent series of 12 months
752 (complete years), using a recursive procedure[54]. Monthly CWD estimation begins with the wettest
753 month of the first year in the interval, and is calculated as 100 mm per month evapotranspiration (ET)
754 minus monthly precipitation (P). Then, CWD values for the subsequent 11 months were calculated
755 recursively as: $CWD_i = ET - P_i + CWD_{i-1}$ (equation 4), where negative CWD_i values were set to
756 zero[54] (no drought conditions). This procedure was repeated for each subsequent complete 12 months.
757 Then, we calculate the annual MCWD as the largest monthly CWD value for every subsequent
758 complete year within the census interval. Finally the MCWD of a census interval is calculated as the
759 mean of the annual MCWD values within the census interval. MCWD is an easily interpretable drought
760 metric: larger values indicate more severe water deficits.
761

To calculate the environmental change of potential predictor variables, CO_2-change, MAT-change and MCWD-change, we selected an optimum period over which to calculate the change. We derived this optimum period empirically by assessing the correlation of carbon gains (all plots, all censuses) with the change in each environmental variable, using linear mixed effects models (lmer function in R, lme4 package[50]). The annualised change in the environmental variable was calculated as the change between the focal interval and a prior interval (termed the baseline period) with a lengthening time window ranging from 1 year through to 80 years prior to the focal interval (i.e. 80 linear mixed effects models per variable). We calculated AIC for each model and selected the interval length with the lowest AIC. Thus, MAT-change (in °C yr^{-1}) $= \frac{(MAT_i - MAT_b)}{(date_i - date_b)}$ (equation 5), where MAT_i is the MAT over the focal census interval calculated using the procedure described above, MAT_b is the MAT over a baseline period prior to the focal interval, $date_i$ is the mid-date of the focal census interval and $date_b$ is the mid-date of the baseline period. The lmer results show that MAT-change (in °C yr^{-1}) is the difference between the focal interval and the mean MAT over the prior 5 years; CO_2-change is the difference between the focal interval and the mean CO_2 over the prior 56 years. MCWD showed no clear trend, so MCWD-change was not included in the models. All three results conform to *a priori* theoretical expectations: see Extended Data Figure 3.

We calculated two forest attributes that may alter responses to environmental change as potential predictor variables: Wood Density (WD) and Carbon Residence Time (CRT). In intact old-growth forests, mean WD (in g cm^{-3}) is inversely related to resource availability[26,60,61], as is seen in our dataset (carbon gains and plot-level mean WD are negatively correlated, Extended Data Figure 4). WD is calculated for each census in the dataset, as the mean WD of all trees alive at the end of the census. Carbon residence time (CRT, in yrs) is a measure of the time that fixed carbon stays in the system. CRT is a potential correlate of the impact of past carbon gains on later carbon losses[28]. To avoid circularity in the models, the equation used to calculate CRT differed depending on the response

787 variable. If the response variable is carbon loss, the CRT equation is based on gains: $CRT = \frac{AGC}{gains}$
788 (equation 6), with AGC for each interval based on AGC at the end of the interval, and the gains for
789 each interval calculated as the mean of the gains in the interval and the previous intervals (i.e. long-
790 term gains). If the response variable is carbon gain, the CRT equation is based on losses: $CRT = \frac{AGC}{losses}$
791 (equation 7). The equation employed for use in the carbon loss model (equation 6) is the standard
792 formula used to calculate CRT and is retained in the minimum adequate model (see below and Table
793 2). The non-standard CRT equation (equation 7) used in the carbon gain model is not retained in the
794 minimum adequate model (see below).
795
796 **Modelling census-level carbon gains and losses**
797 We first construct two models including only the environmental variables: atmospheric carbon dioxide
798 (CO_2), mean annual temperature (MAT), and drought as maximum climatological water deficit
799 (MCWD). One model has carbon gains as the response variable, the other has carbon losses as the
800 response variable (both in Mg C ha^{-1} yr^{-1}). Models were fitted using the lme function in R, with
801 maximum likelihood (NLME package[62]). All census intervals within all plots were used, weighted by
802 plot size and census length (using equation 3). Plot identity was included as a random effect, i.e.
803 assuming that the intercept can vary randomly among plots. All predictor variables in the models were
804 scaled without centering (scale function in R, RASTER package[49]). Carbon gain values were normally
805 distributed but carbon loss values required a power-law transformation ($\lambda = 0.361$) to meet normality
806 criteria. Multi-parameter models are:
807 $carbon\ gains = intcp + a*CO_2 + b*MAT + c*MCWD$ (model 1);
808 $carbon\ losses = intcp + a*CO_2 + b*MAT + c*MCWD$ (model 2);
809 where *intcp* is the estimated model intercept, and *a, b,* and *c* are model parameters giving the slope of
810 relationships with environmental predictor variables. Multi-parameter model outputs for carbon gain
811 and carbon loss are given in Extended Data Table 1. Single-parameter relations are shown in Figure 2.

812

813 The carbon gains model shows significant trends consistent with *a priori* expectations. However, the
814 carbon loss model has no explanatory power (all parameters non-significant, see Figure 2 and Extended
815 Data Table 1), so we further investigated what is driving the trends by constructing two more complex
816 models, including the same environmental predictors (CO_2, MAT, MCWD), plus their rate of change
817 (CO_2-change, MAT-change, MCWD-change), and forest attributes that may alter how forests respond
818 (WD, CRT), as described above. We evaluated the possible inclusion of a differential continent effect
819 of each variable in the full model. We first construct models with only a single predictor variable, and
820 allow different slopes in each continent. Next, if removal of the continent-specific slope (using
821 stepAIC function in R, MASS package[63]) decreased model Akaike Information Criterion (AIC) then
822 the continent-specific slope was not included in the full model for that variable. Only MCWD showed
823 a significant differential continent-specific slope. This implies that forests on both continents have
824 common responses to CO_2-change, MAT, MAT-change, WD and CRT, but respond differently to
825 differences in MCWD. This is most likely because wet-adapted species are much rarer in Africa than
826 in Amazonia as a result of large differences in past climate variation[64]. Lastly, we allowed different
827 intercepts for the two continents, to potentially account for differing biogeographical or other
828 continent-specific factors. For the carbon loss model, we applied the same continent-specific effects
829 for slope as for the carbon gain model, and carbon loss values were transformed using a power-law
830 transformation ($\lambda = 0.361$) to meet normality criteria.

831

832 For both carbon gains and losses we parameterized full models including the significant continent-
833 specific effect of MCWD and simplified models using the stepAIC function in R, which sequentially
834 removes terms until there are no terms that reduce model AIC after removal. As such, the minimum
835 adequate models are:

*carbon gains=intcp*continent +a*CO_2-change+b*MAT+c*MAT-change+d*MCWD*continent+e*WD* (model 3);

carbon losses=intcp+aCO_2-change+b*MAT-change+c*MCWD+d*CRT* (model 4).

Parameters of these minimum adequate models for carbon gain and carbon loss are given in Table 2. CRT was retained in the carbon loss model, and WD was retained in the carbon gain model. These results are expected *a priori* because growth is likely primarily impacted by resource availability, while losses are likely primarily impacted by how long fixed carbon is retained in the system.

Predicting the future carbon gain, loss and the net carbon sink

We used estimates of the predictor variables and the parameters of the minimum adequate gain and loss models (Table 2) to estimate the mean gains and losses for the plot networks in Africa and Amazonia from 1983 through to 2040, with the net carbon sink per unit area obtained by subtracting the losses from the gains (seen in Figure 3). For predictor variables in the past, we calculated annual records for CO_2-change, MAT, MAT-change, MCWD, WD and CRT for each plot location from 1983 to 2015, as described above (mean trends shown in Extended Data Figure 5). For predictor variables in the future, we used the annual records from 1983 to 2015 to parameterize a continent-specific linear regression for CO_2-change, MAT, MAT-change, MCWD, WD, and CRT, which is used to estimate predictor variables for each plot location from 2015 to 2040 (mean trends shown in Extended Data Figure 5). Predicted mean annual gains and losses for 1983 to 2040 are calculated by multiplying model parameters by annual values of the corresponding predictor variables. Model prediction uncertainty is derived from model parameters multiplied by each predictor variable value ±1σ. To obtain total continental sink values in the future (Table 1), per unit area sink estimates were multiplied by future forest area, using the area in each continent from 1990-2010 and an exponential model for each continent to estimate each continents' forest area in 2020, 2030 and 2040 (see Continental and pan-tropical carbon sink estimates, above).

Extended Data

Extended Data Table 1. Models based on environmental variables alone to predict carbon gains and losses in African and Amazonian tropical forests. Where continental values differ, those for Africa are reported first, followed by Amazon values. Significant values in **bold**.

Carbon gains, Mg C ha^{-1} yr^{-1}					
Predictor variable	**Parameter value**	**Standard Error**	**t-value**	**p-value**	**2000-2015 change in gains (%) ***
(Intercept)	**4.694**	0.733	6.402	<0.001	-
CO_2 (ppm)	**0.005**	0.001	3.186	0.001	5.78% | 5.90%
MAT (°C)	**-0.143**	0.021	-6.928	<0.001	-1.24% | -1.89%
MCWD (mm x1000)	**-1.164**	0.207	-5.628	<0.001	-1.42% | -2.08%
Carbon losses, Mg C ha^{-1} yr^{-1} †					
Predictor variable	**Parameter value**	**Standard Error**	**t-value**	**p-value**	**2000-2015 change in losses (%) ***
(Intercept)	1.033	1.855	0.557	0.578	-
CO_2 (ppm)	0.004	0.004	0.949	0.343	6.60% | 5.83%
MAT (°C)	-0.015	0.044	-0.343	0.732	-0.18% | -0.24%
MCWD (mm x1000)	-0.515	0.499	-1.032	0.302	-0.86% | -1.09%

***** The 2000-2015 change in gains/losses for each predictor variable was estimated allowing only the focal predictor to vary; this change was then expressed as a percentage of the annual gains/losses in the year 2000 allowing all predictors to vary.

† carbon loss values were normalized via power-law transformation, $\lambda = 0.361$.

872 **Extended Data Table 2. Forest area estimates used to calculate total continental forest sink.**

Period	intact forest area (Mha) *		
	Africa	**Amazon**	**Southeast Asia**
1980	671.5	958.3	233.6
1990	600.2	885.2	190.6
2000	531.8	817.2	136.9
2010	477.8	756.3	118.4
2015	450.5	726.7	101.5
2020	425.5	698.5	90.1
2030	379.7	645.4	71.0
2040	338.8	596.4	56.0

873 * Intact forest area for 1990, 2000 and 2010 is published in ref.[1] (i.e. the total forest area minus forest regrowth);
874 to estimate intact forest area for 1980, 2015, 2020, 2030 and 2040 we fitted exponential models for each
875 continent using the 1990-2010 data.

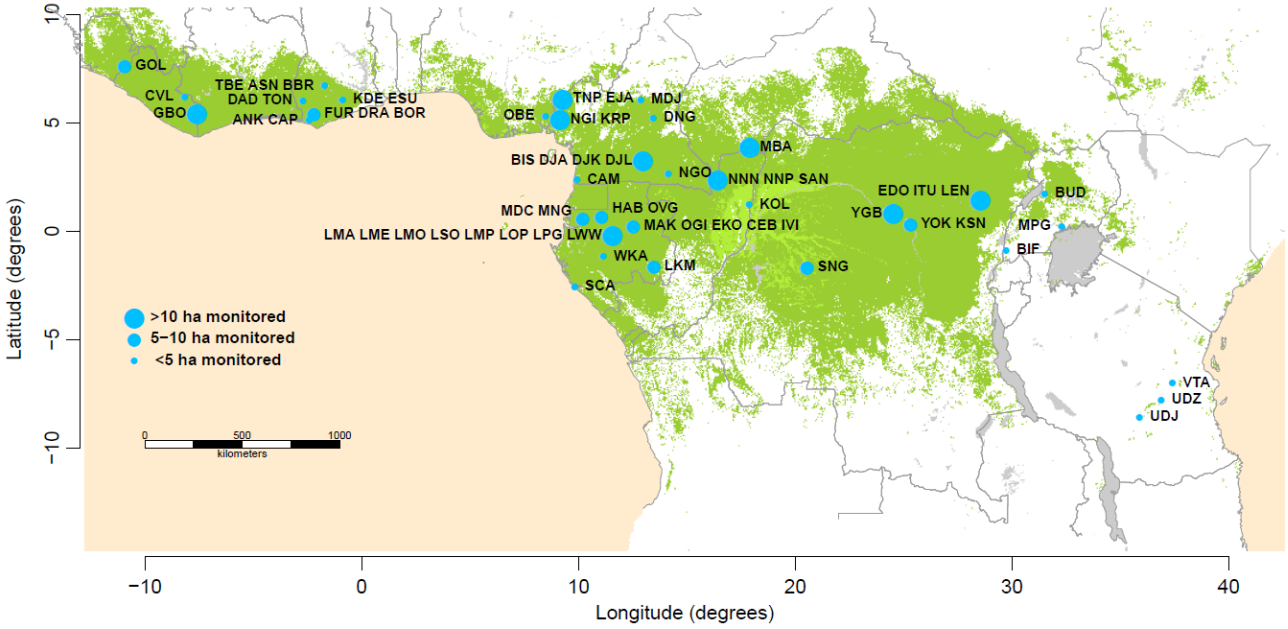

Extended Data Figure 1. Map showing the locations of the 244 plots included in this study. Dark green represents all lowland closed-canopy forests, submontane forests and forest-agricutlure mosaics; light green shows swamp forests and mangroves[65]. The three-letter codes refer to plot-cluster names (see Supplementary Table 1 for the full list of plots). Clusters <50 km apart are shown as one dot for display only. Blue dot size corresponds to sampling effort in terms of hectares monitored.

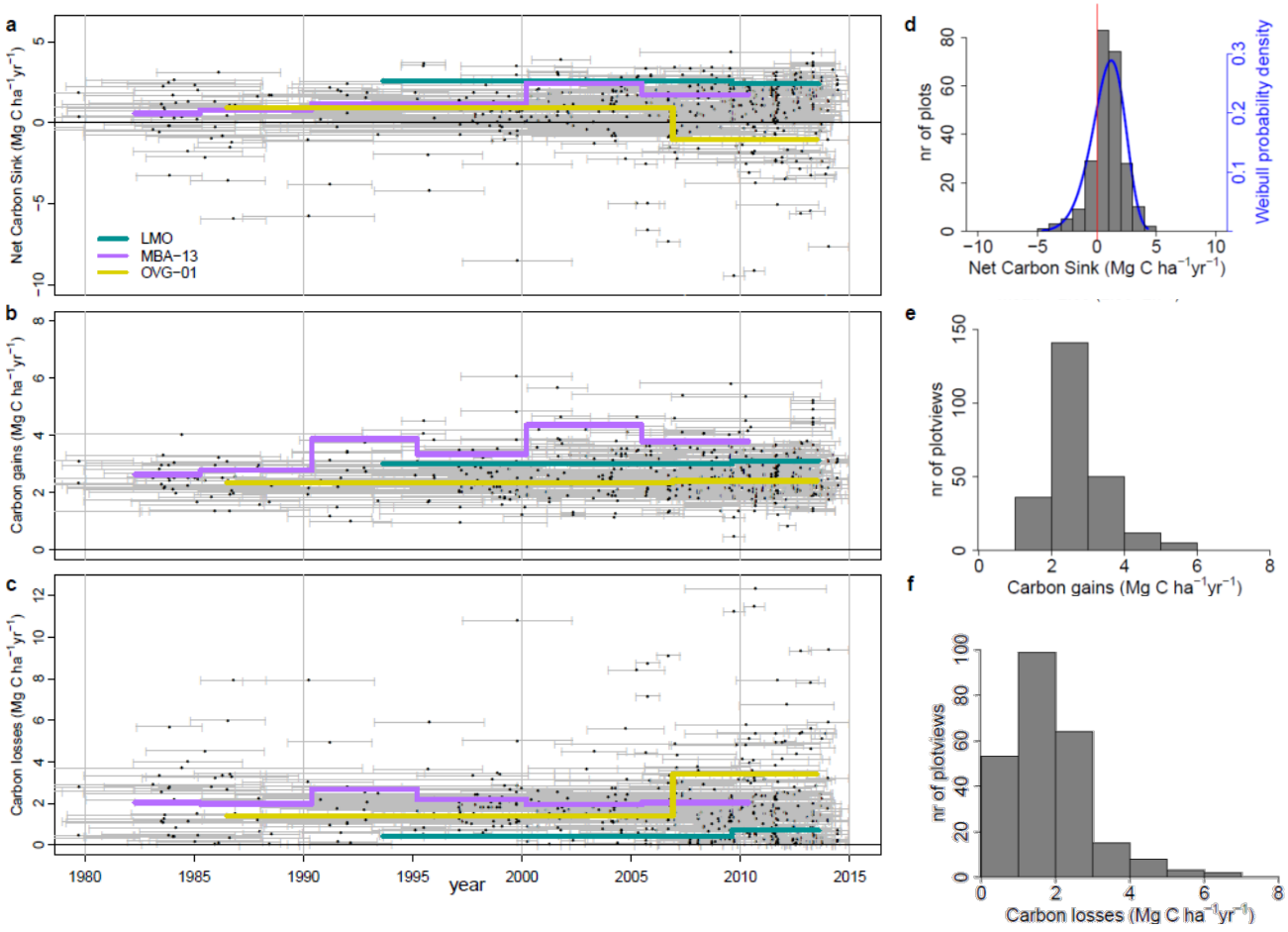

Extended Data Figure 2. Distribution of values of the long-term above-ground carbon dynamics of 244 African intact tropical forest inventory plots. Points in the scatterplots indicate the mid-census interval date, with horizontal bars connecting the start and end date for each census interval for the net carbon sink (**a**), carbon gains (from woody productivity) (**b**), and carbon losses (from mortality) (**c**). Examples of time series for three individual plots are shown in purple, yellow and green. Associated histograms show the distribution of the plot-level net carbon sink (**d**) (with a three-parameter Weibull probability density distribution fitted in blue, showing the sink is significantly larger than zero; one-tail t-test: $p<0.001$), carbon gains (**e**), and carbon losses (**f**).

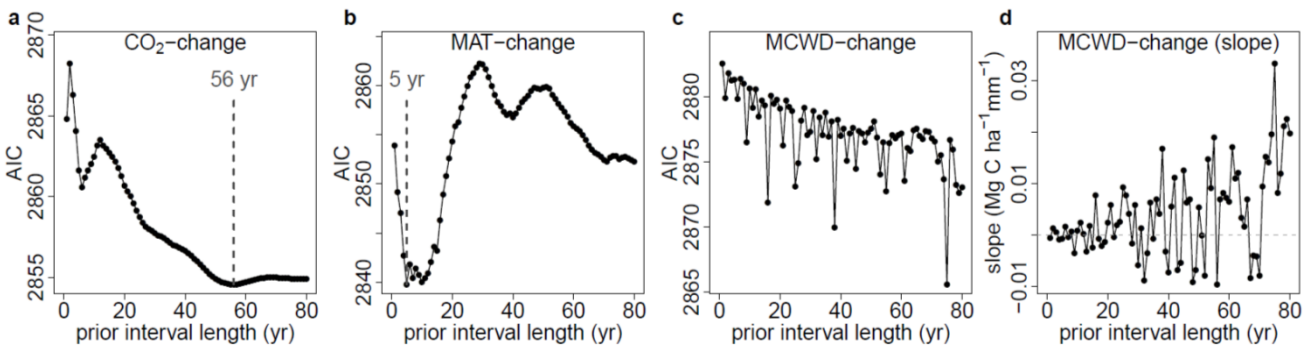

Extended Data Figure 3. Akaike's Information Criterion (AIC) from correlations between the carbon gain in tropical forest inventory plots and changes in either atmospheric CO_2, temperature (as MAT) or drought (as MCWD) each calculated over ever-longer prior intervals. Panels show AIC from linear mixed effects models of carbon gains and, atmospheric CO_2 (CO_2-change) (**a**), Mean Annual Temperature (MAT-change) (**b**), and Maximum Climatological Water Deficit (MCWD-change, *n*=565 plots) (**c**). For CO_2 the AIC minimum was observed when predicting the carbon gain from the change in CO_2 calculated over a 56 year long prior interval length. We use this length of time to calculate our CO_2-change parameter. Such a value is expected *a priori* because forest stands will respond most strongly to CO_2 when most individuals have grown under the new rapidly changing conditon, which should be at its maximum at a time approximately equivalent to the carbon residence time of a forest stand[66,67] (a mean of 62 years in this dataset). For MAT the AIC minimum was 5 years, which we use as the prior interval to calculate our MAT-change parameter. This length is consistent with experiments showing temperature acclimation of leaf-level and plant-level photosynthetic and respiration processes over half-decadal timescales[29,68]. For MCWD the AIC minimum is not obvious, while the slope of the correlation, shown in panel (**d**), has no overall trend and oscillates between positive or negative values, meaning there is no obvious relationship between carbon gains and the change in MCWD over intervals longer than 1 year; thus MCWD-change is not included in our models. This result is expected, because once a drought ends, its impact on tree growth fades rapidly[12,69], hence lagged impacts of past droughts are not expected.

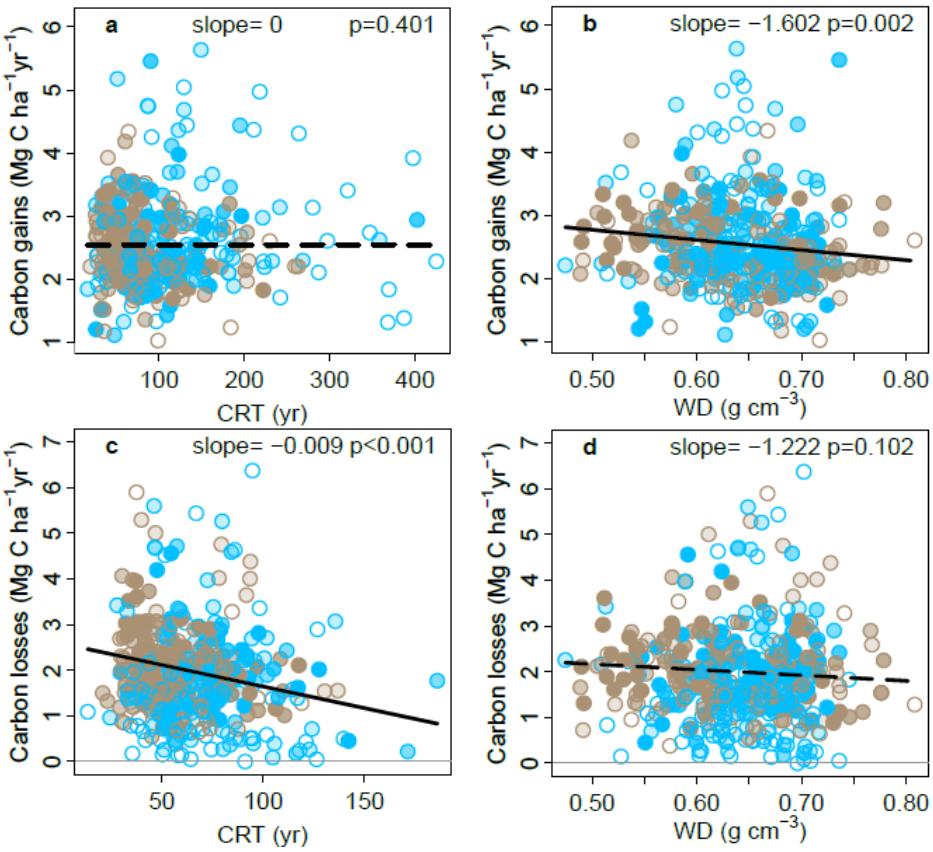

Extended Data Figure 4. Potential forest-dynamics-related drivers of carbon gains and losses in structurally intact old-growth African and Amazonian tropical forests. The aboveground carbon gains, from woody productivity (**a-b**), and aboveground carbon losses, from mortality (**c-d**), are plotted against the carbon residence time (CRT), and wood density (WD), for African (blue) and Amazonian (brown) inventory plots. Linear mixed effect models were performed with census intervals (n=1566) nested within plots (n=565) to avoid pseudo-replication, using an empirically derived weighting based on interval length and plot area (see methods). Significant regression lines for the complete dataset are shown as a solid line; non-significant regressions as a dashed line. Each dot represents a time-weighted average plot-level value; transparency of the inner part of the dot represents total monitoring length, with empty circles corresponding to plots monitored for ≤ 5 years and solid dots for plots monitored for >20 years. Carbon loss data are presented untransformed for clarity; linear mixed effects models on transformed data to fit normality assumptions do not change the results. For the carbon gains and losses models CRT is calculated differently: see methods.

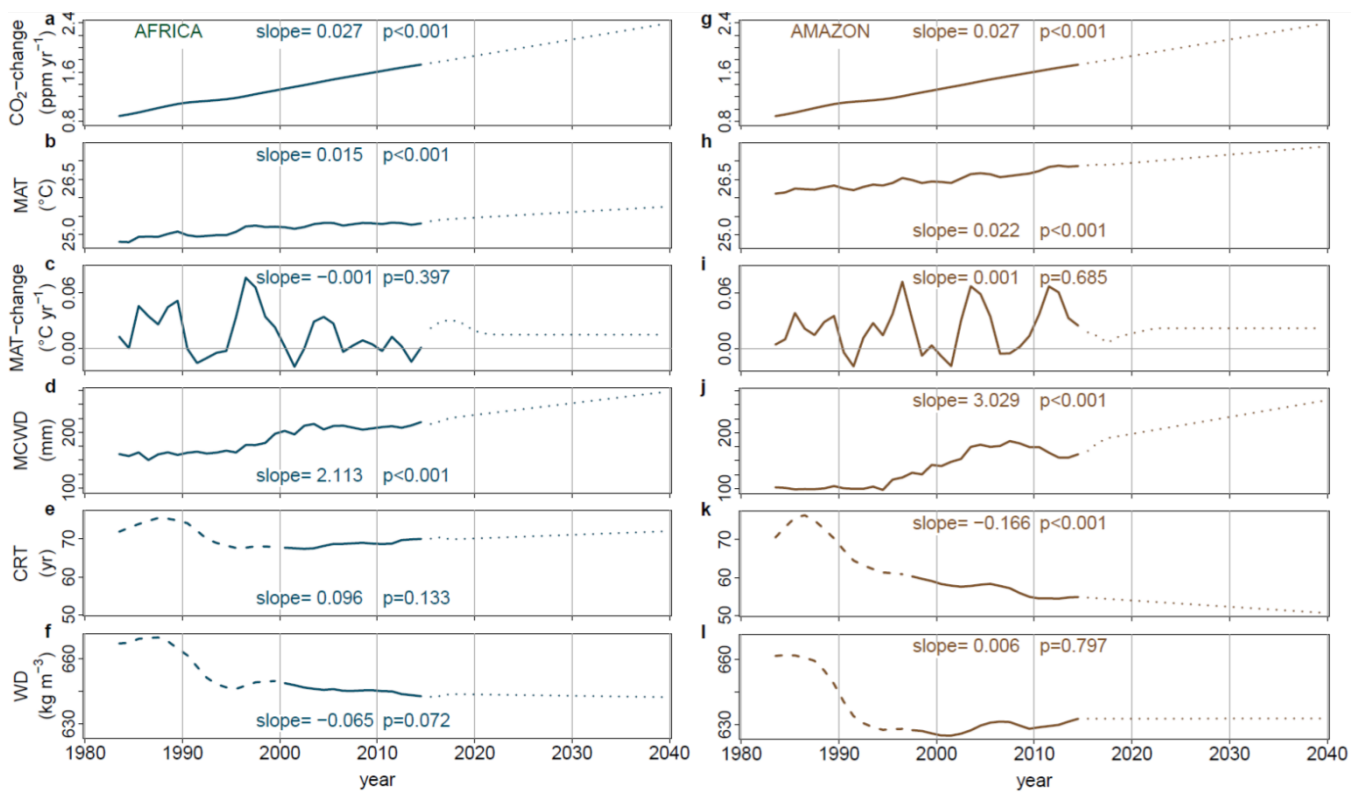

Extended Data Figure 5. Trends in predictor variables used to estimate long-term trends in above-ground carbon gains, carbon losses and the resulting net carbon sink in African and Amazonian tropical forest plot networks. Solid lines, blue for Africa (**a-f**), brown for Amazonia (**g-l**), are the mean annual value for all plot locations on each continent, from published datasets (CO_2-change, MAT, MAT-change, MCWD), or estimated from the plot data (WD, CRT). Dotted lines are future values estimated from linear trends on the 1983-2014 data (slope and p-value reported in each panel). Trends for environmental variables (CO_2-change, MAT, MAT-change, MCWD) are from simple linear models using the mean annual record. Trends for CRT and WD are from linear mixed effects models using the plot data, i.e. regressing the mid-point of each census interval against the value of the predictor variable for that census interval, using plot identity as a random effect, and weighting observations by plot size and census interval length (as in Figure 1). Dashed lines in panels e-f and k-l represent the time window where <75% of plots were monitored, hence contributing less to the linear mixed effects model.

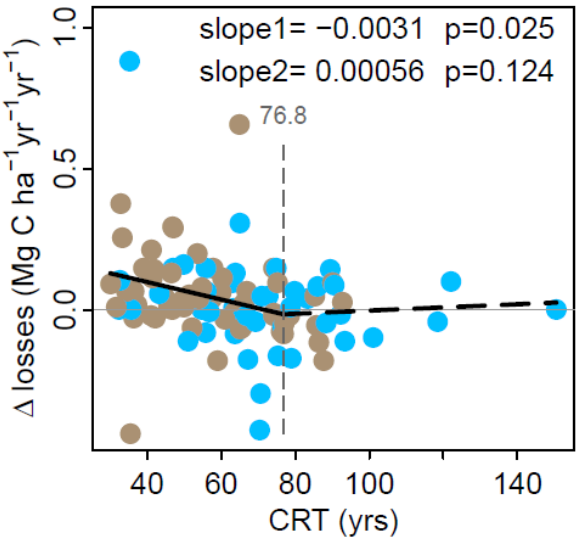

Extended Data Figure 6. The change in carbon losses versus carbon residence time (CRT) of plots in Africa and Amazonia. The data include only plots monitored for >20 years (i.e. roughly one-third of the mean CRT of the pooled African and Amazon dataset; n = 116). Breakpoint regression was used to assess the CRT length below which forest carbon losses begin to increase. Plots with CRT <77 years show a long-term increase in carbon losses. Blue dots are African plots, brown dots are Amazonian plots.

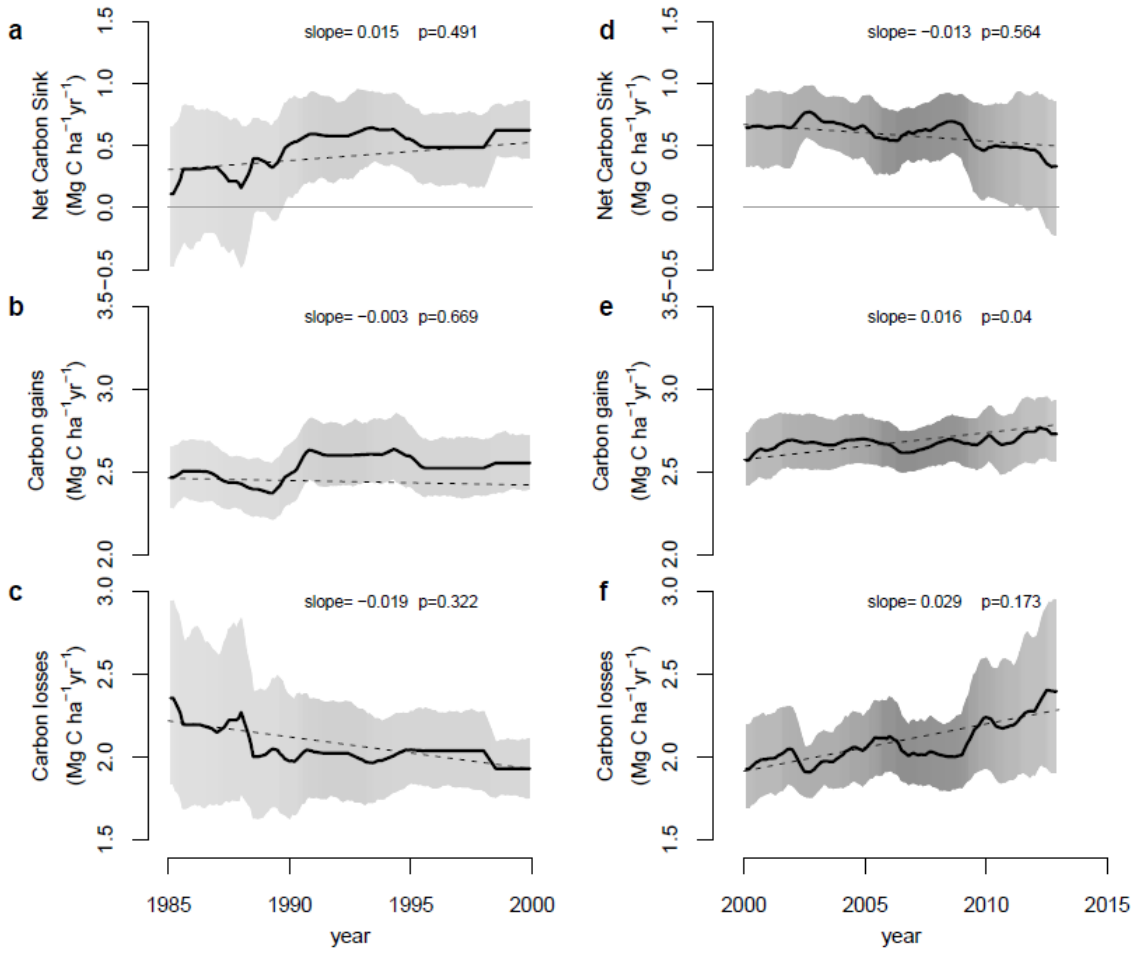

Extended Data Figure 7. Trends in African forest net aboveground live biomass carbon sink, carbon gains and carbon losses, calculated for the last 15 years of the twentieth century (left panels a-c) and the first 15 years of the twenty-first century (right panels d-f). Plots were selected from the full dataset if their census intervals covered at least 50% of the respective time windows (*n*=56 plots for 1985-2000, and *n*=134 plots for 2000-2015, respectively). Solid lines show mean values calculated as for Figure 1; shading corresponds to the 95% CI. Dashed lines, slopes and p-values are from linear mixed effects models.

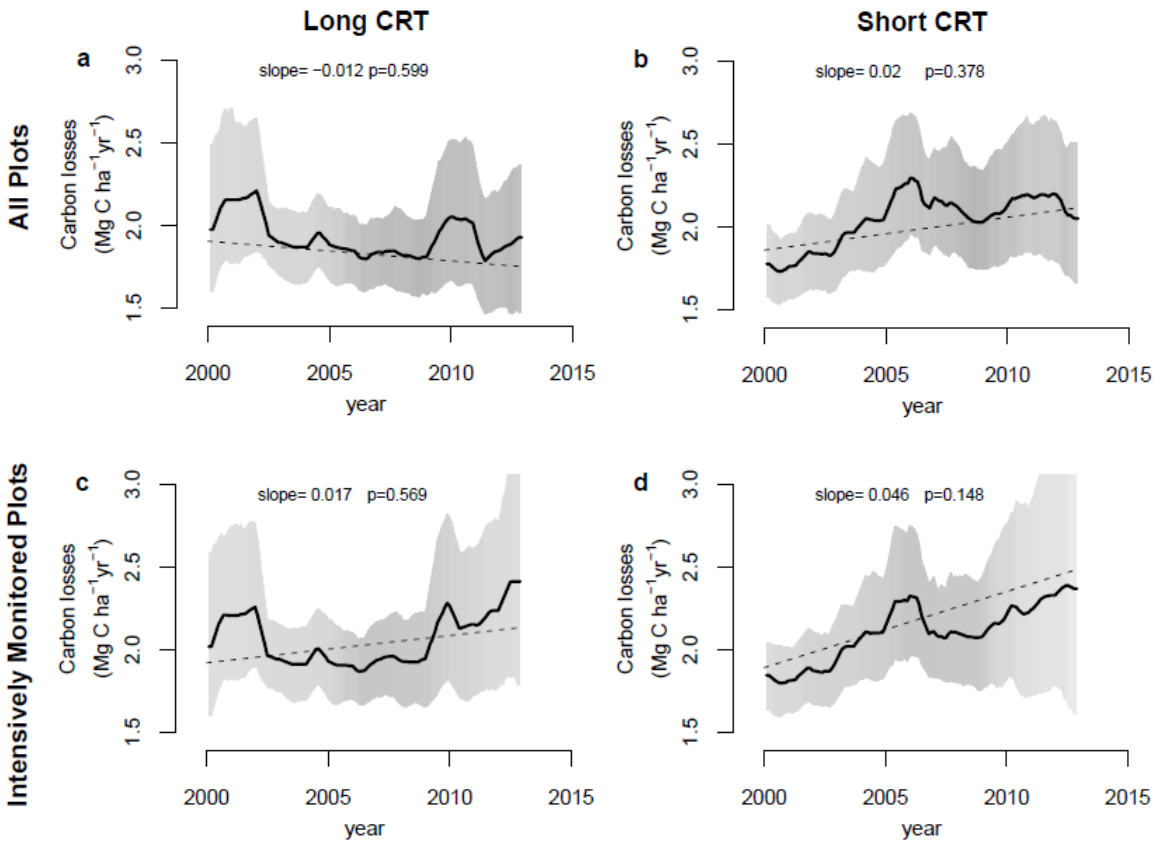

Extended Data Figure 8. Twenty-first century trends in aboveground biomass carbon losses from African tropical forest inventory plots with either long (left panels) or short (right panels) carbon residence time. Upper panels include all plots, i.e. as in Figure 1, but split into a long-CRT group (**a**), and a short-CRT group (**b**), each containing half the 244 plots. Lower panels restrict plots to those spanning >50% of the time window, i.e. as in Extended Data Figure 7, but split into a long-CRT group (**c**), and a short-CRT group (**d**), each containing half the 134 plots. Solid lines indicate mean values, shading the 95% CI. Dashed lines, slopes and p-values are from linear mixed-effects models. Carbon losses increase more through time in the short-CRT than the long-CRT group of plots, in both datasets, although this increase is not statistically significant.

References (Methods only)

31 Hijmans, R. J., Cameron, S. E., Parra, J. L., Jones, P. G. & Jarvis, A. Very high resolution interpolated climate surfaces for global land areas. *International Journal of Climatology* **25**, 1965-1978, doi:10.1002/joc.1276 (2005).

32 Lopez-Gonzalez, G., Lewis, S. L., Burkitt, M. & Phillips, O. L. ForestPlots.net: a web application and research tool to manage and analyse tropical forest plot data. *Journal of Vegetation Science* **22**, 610–613, doi:10.1111/j.1654-1103.2011.01312.x (2011).

33 Sheil, D. & Bitariho, R. Bwindi Impenetrable Forest TEAM Site. Data Set Identifier: TEAM-DataPackage-20151201235855_1254. (2009).

34 Kenfack, D. Korup National Park TEAM Site. Data Set Identifier: TEAM-DataPackage-20151201235855_1254. (2011).

35 Rovero, F., Marshall, A. & Martin, E. Udzungwa TEAM Site. Data Set Identifier: TEAM-DataPackage-20151130235007_5069. (2009).

36 Hockemba, M. B. N. Nouabalé Ndoki TEAM Site. Data Set Identifier: TEAM-DataPackage-20151201235855_1254. (2010).

37 Anderson-Teixeira, K. J. *et al.* CTFS-ForestGEO: a worldwide network monitoring forests in an era of global change. *Global Change Biology* **21**, 528-549, doi:10.1111/gcb.12712 (2015).

38 Gourlet-Fleury, S. *et al.* Tropical forest recovery from logging: a 24 year silvicultural experiment from Central Africa. *Philosophical Transactions of the Royal Society B-Biological Sciences* **368**, 20120302, doi:10.1098/rstb.2012.0302 (2013).

39 Phillips, O., Baker, T., Brienen, R. & Feldpausch, T. RAINFOR field manual for plot establishment and remeasurement. Available at http://www.rainfor.org/upload/ManualsEnglish/RAINFOR_field_manual_version_2016.pdf. (2016).

40 Talbot, J. *et al.* Methods to estimate aboveground wood productivity from long-term forest inventory plots. *Forest Ecology and Management* **320**, 30-38, doi:10.1016/j.foreco.2014.02.021 (2014).

41 Lopez-Gonzalez, G., Hubau, W., Pickavance, G., Lewis, S. & Phillips, O. Forestplots.net Manual. Available at http://www.forestplots.net/upload/ManualsEnglish/ForestPlotsManualApril112016_sm.pdf. (2016).

42 Sullivan, M. J. P. *et al.* Field methods for sampling tree height for tropical forest biomass estimation. *Methods in Ecology and Evolution* **9**, 1179-1189, doi:10.1111/2041-210X.12962 (2018).

43 Lopez-Gonzalez, G., Sullivan, M. & Baker, T. BiomasaFP package. Tools for analysing data downloaded from ForestPlots.net. R package version 0.2.1. Available at http://www.forestplots.net/en/resources/analysis. (2017).

44 Feldpausch, T. R. *et al.* Tree height integrated into pantropical forest biomass estimates. *Biogeosciences* **9**, 3381-3403, doi:10.5194/bg-9-3381-2012 (2012).

45 Chave, J. *et al.* Towards a worldwide wood economics spectrum. *Ecology Letters* **12**, 351-366, doi:10.1111/j.1461-0248.2009.01285.x (2009).

46 Zanne, A. E. *et al. Data from: Towards a worldwide wood economics spectrum* (Dryad Digital Repository, 2009).

47 Chave, J. *et al.* Improved allometric models to estimate the aboveground biomass of tropical trees. *Global Change Biology* **20**, 3177-3190, doi:10.1111/gcb.12629 (2014).

48 Martin, A. R., Doraisami, M. & Thomas, S. C. Global patterns in wood carbon concentration across the world's trees and forests. *Nature Geoscience* **11**, 915-920, doi:10.1038/s41561-018-0246-x (2018).

49 R Development Core Team. R: A Language and Environment for Statistical Computing. Available at http://www.R-project.org/. (2015).

50 Bates, D., Maechler, M., Bolker, B. & Walker, S. lme4: Linear mixed-effects models using Eigen andS4.Rpackage version, 1.0-4. Available at http://www.inside-r.org/packages/lme4/versions/1-0-4. (2013).

51 Fox, J. *Applied Regression Analysis and Generalized Linear Models*. Second edn, (Sage Publishing, 2008).

52 Chave, J. *et al.* Assessing evidence for a pervasive alteration in tropical tree communities. *PLoS Biology* **6**, 0455-0462, doi:10.1371/journal.pbio.0060045 (2008).

53 Yuen, J. Q., Ziegler, A. D., Webb, E. L. & Ryan, C. M. Uncertainty in below-ground carbon biomass for major land covers in Southeast Asia. *Forest Ecology and Management* **310**, 915-926, doi:10.1016/j.foreco.2013.09.042 (2013).

54 Aragão, L. E. O. C. *et al.* Environmental change and the carbon balance of Amazonian forests. *Biological Reviews* **89**, 913-931, doi:10.1111/brv.12088 (2014).

55 Tans, P. & Keeling, R. Mauna Loa CO_2 monthly mean data. Available at http://www.esrl.noaa.gov/gmd/ccgg/trends/. (2016).

56 Harris, I., Jones, P. D., Osborn, T. J. & Lister, D. H. Updated high-resolution grids of monthly climatic observations – the CRU TS3.10 Dataset. *International Journal of Climatology* **34**, 623–642 doi:10.1002/joc.3711 (2014).

57 Schneider, U. *et al.* GPCC Full Data Reanalysis Version 6.0 at 0.5°: Monthly Land-Surface Precipitation from Rain-Gauges built on GTS-based and Historic Data. doi:10.5676/DWD_GPCC/FD_M_V6_050 (2011).

58 Sun, Q. *et al.* Review of Global Precipitation Data Sets: Data Sources, Estimation, and Intercomparisons. *Reviews of geophysics* **56**, 79-107, doi:10.1002/ (2017).

59 Huffman, G. J. *et al.* The TRMM Multisatellite Precipitation Analysis (TMPA): Quasi-Global, Multiyear, Combined-Sensor Precipitation Estimates at Fine Scales. *Journal of Hydrometeorology* **8**, 38-55, doi:10.1175/jhm560.1 (2007).

60 Quesada, C. A. *et al.* Variations in chemical and physical properties of Amazon forest soils in relation to their genesis. *Biogeosciences* **7**, 1515-1541, doi:10.5194/bg-7-1515-2010 (2010).

61 Baker, T. R., Swaine, M.D., Burslem, D.F.R.P. Variation in tropical forest growth rates: combined effects of functional group composition and resource availability. *Perspectives in Plant Ecology, Evolution and Systematics* **6**, 21-36, doi:10.1078/1433-8319-00040 (2003).

62 Pinheiro, J. C. & Bates, D. M. *Mixed-Effects Models in S and S-PLUS.* First edn, 528 (Springer, 2000).

63 Venables, W. N. & Ripley, B. D. *Modern Applied Statistics with S.* Fourth edn, 498 (Springer, 2002).

64 Parmentier, I. *et al.* The odd man out? Might climate explain the lower tree alpha-diversity of African rain forests relative to Amazonian rain forests? *Journal of Ecology* **95**, 1058-1071 (2007).

65 Mayaux, P., De Grandi, G. & Malingreau, J.-P. Central African Forest Cover Revisited: A Multisatellite Analysis. *Remote Sensing of Environment* **71**, 183–196, doi:10.1016/S0034-4257(99)00073-5 (2000).

66 Lloyd, J. & Farquhar, G. D. The CO_2 dependence of photosynthesis , plant growth responses to elevated atmospheric CO_2 concentrations and their interaction with soil nutrient status . I . General principles and forest ecosystems. *Functional Ecology* **10**, 4-32, doi:10.2307/2390258 (1996).

67 Galbraith, D. *et al.* Residence times of woody biomass in tropical forests. *Plant Ecology & Diversity* **6**, 139-157, doi:10.1080/17550874.2013.770578 (2013).

68 Aspinwall, M. J. *et al.* Convergent acclimation of leaf photosynthesis and respiration to prevailing ambient temperatures under current and warmer climates *in Eucalyptus tereticornis*. *New Phytologist* **212**, 354-367, doi:10.1111/nph.14035 (2016).

69 Bonal, D., Burban, B., Stahl, C., Wagner, F. & Hérault, B. The response of tropical rainforests to drought—lessons from recent research and future prospects. *Annals of Forest Science* **73**, 27-44, doi:10.1007/s13595-015-0522-5 (2016).